FABRICATION AND CHARACTERIZATION OF Pd/n-Si SCHOTTKY CONTACTS

A Thesis Submitted
in Partial Fulfilment of the Requirements
for the Degree of

Master of Technology

by

Pragya Tripathi

to the

Materials Science Programme
Indian Institute of Technology, Kanpur
August, 1997

This t

Fabricati

by Pragy

has not b

August, 19

CERTIFICATE

This is to certify that the work contained in the thesis entitled **Fabrication and Characterization of Pd/n-Si Schottky Contacts** *by* **Pragya Tripathi** *has been carried out under my supervision and has not been submitted elsewhere for a degree.*

Jitendra Kumar

August, 1997

Jitendra Kumar
Professor
Materials Science Programme
Indian Institute of Technology
Kanpur - 208016

Acknowledgements

I wish to express my deep sense of gratitude to Professor Jitendra Kumar who played the key role in bringing about the success of this work. The successful completion has been possible only due to his lively guidance, intellectual support, meticulous observations and critical analysis.

I wish to thank Prof. K.N. Rai for allowing me to use the cryostat alongwith the close cycle helium refrigerator system.

I 'm grateful to Dr. Subhash Chand for helping me in getting acquainted with various instruments and guiding me in understanding the theoretical aspects

I'm thankful to Ruchi, Sanjil and Renu for their invaluable help .

Thanks are due also to my lab colleagues Madhukar, Tayyab, Lakhmani, D.K. and Prasad. I sincerely appreciate the cooperation given by my classmates and friends throughout my M.Tech. programme. I acknowledge the immense help received from all the officers and staff members of Materials Science Programme and Advanced Centre for Materials Science.

Lastly, I would like to thank my family members for being a constant source of encouragement throughout this work.

Pragya Tripathi

Pragya Tripathi

Abstract

Pd/n-Si Schottky contacts have been fabricated by depositing a palladium film of $\sim$ 80 nm thickness in vacuum $\sim 10^{-6}$ m[illegible], using an electron beam evaporation source onto a cleaned n-type <111> silicon wafer and subsequent vacuum annealing at 200°C-500°C for different lengths of time. Their current- voltage (I-V) characteristics have been measured in the temperature range 80K-300K and analysed on the basis of the thermionic emission-diffusion(TED) mechanism and parameters, viz.,barrier height , ideality factor , saturation current etc. are determined. The zero bias barrier height (ϕ_{bo}) is found to decrease while ideality factor(η) increases with decrease in temperature. Further , the changes in ϕ_{bo} and η are quite significant at low temperatures. This abnormal behaviour has been explained by invoking the concept of barrier inhomogeneities and describing them by double Gaussian distribution of barrier heights with parameters as : zero bias mean barrier height (ϕ_{bo}) 0.93V and 0.63V, standard deviation (σ_o) 11.2 and 67 6mV in the temperature range 165-300K and 80-165K, respectively.

It is shown that thermal annealing at 400°C , 450°C and 500°C of Pd/n-Si invariably leads to the formation of silicide of composition Pd_2Si possessing hexagonal structure (Fe_2P type) with parameters a=13.055$\AA$, c=27.49$\AA$. Also the growth occurs preferentially in certain directions such that (11.4) or (00.1) planes of hexagonal Pd_2Si lie parallel to the underlying (111) Si substrate in the beginning, but, shows polycrystallinity with time at all the temperatures. The reflectance is shown to usually decrease with the growth of Pd_2Si. In the intermediate stages a slight increase in reflectance observed in particular cases is attributed to the disposition of Pd_2Si preferentially on the underlying (111) Si substrate . As the time lapses , Pd_2Si layer exhibits polycrystallinity at all the temperatures and

corresponding reflectance decreases - taking a constant value eventually.

Finally, simulation studies have demonstrated the dominance of TED mechanism for current transport through the Pd/n-Si Schottky contacts. Also, negative temperature coefficients of mean ($\phi_{b\infty}$) and variance (σ_o^2) of the Gaussian distribution function (representing the barrier inhomogeneities at the Schottky contact) are shown to have opposite effects on the temperature dependence of apparent barrier height . While the former causes decrease in barrier height , the later compensates the change by a fixed amount. The overall effect is that Gaussian distribution function shifts towards lower barrier height and at the same time become narrower with rise in temperature, i.e., effective reduction in barrier inhomogeneities occurs.

Contents

Certificate ii
Acknoledgements iii
Abstract iv
Contents vi
List of Figures vii
List of Tables x

1 The Schottky Barrier **1**
1.1 Introduction 1
1.2 The formation of a Schottky barrier 1
1.3 Surface and Interface states 5
1.4 Conduction Mechanisms 10
1.4.1 Thermionic emission-diffusion Mechanism 11
1.4.2 Tunneling through the Barrier 13
1.4.3 Carrier Generation and Recombination 14
1.4.4 Minority Carrier Injection 15
1.5 Methods of Barrier Height Measurement 16
1.6 Importance and Applications 18
1.7 Objective of the present work 19

2 Experimental **21**
2.1 Fabrication of Schottky diodes 21
2.2 Setup for I-V-T measurements 22
2.3 Phase identification microstructure and reflectance measurements . . 22

3 Results and Discussions **25**
3.1 Forward I-V characteristics 25
3.1.1 Zero bias barrier height , ideality factor and series resistance 25
3.1.2 Activation Energy Plot 26
3.2 Concept of Barrier Inhomogenities 26
3.3 Interpretation of the Experimental Data 31
3.4 Evidence for a Double Distribution 33
3.5 X-ray Diffraction Studies 39
3.6 Reflectance measurements and SEM studies 47

4 Simulation Studies **53**
4.1 I-V characteristics 53
4.2 Temperature dependence of barrier height 62

5 Conclusions **67**

List of Figures

1.1 Schematic diagram of band bending before and after metal-semiconductor contact (a)High workfunction metal and n-type semiconductor, i.e.,$\phi_m > phi_s$,(b)low workfunction metal and n-type semiconductor,(c) High workfunction metal and p-type semi conductor,(d) Low workfunction metal and p-type semiconductor. 3

1.2 (a) Qualitative explanation of the origin of surface states in the tight binding picture.Depending on their origin,these states have acceptoror donar like charging character .(b)Electron energy band diagram of n-type semiconductor with surface states (i)under flat band ,(ii) in thermal equillibrium with the bulk,(c)in contact with metal 6

1.3 Origin of metal induced gap states at MS interface (a) dispersion curve of 1D model of semiconductor ;the real band structure with $E_c(k)$ and $E_v(k)$ as conduction and valence bands respectively. $\mathcal{D}_{vs}$ is density of the virtual states (b)Tailing of metal Bloch state into semiconductor 8

1.4 Barrier heights of Si Schottky contacts vs metal workfunction.For comparision the predictions of the Schottky (no interface states) and the Bardeen (high density of interface states) model are given. 9

1 5 Band diagram of a metal semiconductor junction in which the interface region (width$\sim 5\mathring{A}$) is taken into account explicitly. 10

1.6 Transport processes in a forward biased Schottky contact. 11

1.7 Field and thermionic field emission under forward bias 13

1.8 Activation energy plots for determination of barrier height. 16

1.9 $1/C^2$vs applied voltage for determination of barrier height 17

2.1 Block diagram of automated set-up for I-V measurements of Schottky diode over a wide temperature range. 23

2.2 The circuit diagram for I-V measurements of a Schottky diode. 24

3.1 Current-voltage characteristics of Pd/n-Si Schottky contacts in the temperature range (a) 300K-180K (b)165K-80K 27

3.2 Variation of the zero-bias barrier height (ϕ_{bo}) (ϕ_b^f) with temperature in the range 80K-300K. 28

3.3 Temperature dependence of the ideality factor for Pd/n-Si Schottky contacts in the range 80K-300K. Notice the sharp increase in η at low temperatures. 28

3.4	Temperature dependence of the series resistance (R_s) for Pd/n-Si Schottky contacts in the range 80K-300K Notice the sharp increase in R_s at low temperatures.	29
3.5	The $\ln(I_s/T^2)$ vs 1000/T plots of Schottky contacts with best fit straight line(s) Pd/n-Si in the range 80K-300K It shows non-linearity below 165K.	29
3.6	The modified activation energy plots for σ_o 0.1109V and 0.063V,together with experimental data.The straight lines 1 and 2 indicate best fitting of data in temperature ranges 165K-300K and 80-150K	30
3.7	Current-Voltage characteristics od Pd/n-Si Schottky contacts formed by annealing at 400^oC for 1h,in the temperature range (a) 300K-180K (b)165K-80K	34
3.8	Variation of the zero bias barrier height(ϕ_{bo}^-) with temperature,in the range 80K-300K	35
3.9	Temperature dependence of ideality factor for Pd/n-Si Schottky contacts ,in the range 80K-300K.Notice the sharp increase in η at low temperatures	35
3.10	The barrier height ϕ_{bo} obtained from I-V measurements as a function of inverse temperature.Notice the transition occuring around 150K	36
3.11	The zero bias barrier height) as a function of temperature. Full curves 1 and 2 correspond to ϕ_{ap} calculated using eqn. (3.8) for two distributions having ϕ_{bo} (0.93V and 0.629V) and σ_o (0.112V and 0.0667V)	36
3.12	The inverse ideality factor($1/\eta_{ap}$) vs inverse temperature (1/T) plot.The data shows linear variation in the two temperature ranges with transition around 200K	37
3.13	Conventional activation energy $\ln(I_s/T^2)$ vs 1000/T plot. Notice the deviation from linearity below 180K	37
3.14	The modified activation energy plots for σ_o 0.112 V and , 0.067V together with the experimental data.The straight lines 1 and 2 indicate best fitting of data in temperature ranges 165-300K and 80-150K respectively.	38
3.15	Diffractogram for the as deposited sample .	40
3.16	Diffractogram for the sample annealed at 200°C for different lengths of time.	41
3.17	Diffractogram for the sample annealed at 400°C for different lengths of time.	42
3.18	Diffractogram for the sample annealed at 450°C for different lengths of time.	43
3.19	Diffractogram for the sample annealed at 500°C for different lengths of time.	44

3.20	Reflectance vs wavelength plots for the sample annealed at 400°C for different lengths of time.	48
3.21	Reflectance vs wavelength plots for the sample annealed at 450°C for different lengths of time.	49
3.22	Reflectance vs wavelength plots for the sample annealed at 500°C for different lengths of time.	50
3.23	Scanning electron micrographs ot Pd/n-Si Schottky contacts showing microstructure (a)after annealing at 400°C for 12h (b) after annealing at 450°C for 4h (c)after annealing at 500°C for30 min .	52
4.1	Simulated ln(I) vsV plots for the current due to thermionic emission diffusion process at different temperatures.	54
4.2	Simulated ln(I) vsV plots for the current due to generation recombination process at different temperatures.	56
4.3	Simulated ln(I) vsV plots for the current due to tunneling process at different temperatures.	58
4.4	Simulated ln(I) vsV plots for the current due to tunneling process at 300K.	59
4.5	Simulated ln(I) vsV plot showing the current due to the three mechanisms simultaneously at 300K and 200K.	60
4.6	Apparent barrier height vs temperature plot with α_1 varying from -3 to 3 mV/K and α_2 zero.	64
4.7	Apparent barrier height vs temperature plot with α_1 = -3 mV/K and α_2 varying from -3 to 3mV^2/K.	65
4.8	Apparent barrier height vs temperature plot with α_1 = 3 mV/K and α_2 varying from -3 to 3mV^2/K.	65

List of Tables

3.1 Diffraction peaks for Pd 45
3.2 Diffraction peaks for Pd_2Si 46

Chapter 1
The Schottky Barrier

1.1 Introduction

Within the framework of solid state and interface physics , the solid -solid interface is traditionally studied the most . One reason is the enormous importance of metal-semiconductor (MS) junctions and semiconductor heterojunctions for device physics. The metal-semiconductor junction , also known as Schottky diode , is an active device capable of giving a strong non-linear response under appropriate conditions [1-2]. It is found in many metal semiconductor contacts and the underlying physics forms the basis for their rectifying properties.There have been three major periods of industrial importance for the metal-semiconductor contacts - in early twentith century they were used as radio detectors , then as radar detectors during the second world war and later on as clamping diodes, microwave diodes and gates of microwave transistors[3].

The first metal-semiconductor device was made, during the early days of telegraphy , by pressing a sharp metallic wire to an exposed semiconductor surface,for use as radio-wave detector[3, - 9]. But, they proved to be highly unreliable in their characteristics and were subsequently replaced by reproducible planar metal-semiconductor interface , produced by depositing films under high vacuum , with an uniform contact potential and current distribution over the junction area.

1.2 The formation of a Schottky barrier

An ideal surface essentially is one having atomically sharp profile with no intermixing of the components on the either side , e.g., metal and semiconductor in

case of a MS contact. Its electronic properties are described primarily by the work function ϕ_m of metal , electron affinity χ_s of semiconductor, position of their Fermi levels and band structures. When the two are brought into contact , equilibrium requires that the chemical potential on both the sides of interface should be the same. This means that the Fermi levels in the metal and the semiconductor be aligned.The matching of the Fermi levels requires charge to flow from one side to the other In the process, free electron concentration in the semiconductor near the boundary region decreases and, in turn, causes corresponding shift of the Fermi level. Since, the seperation between the conduction band edge E_C and Fermi level E_F increases with decrease in electron concentration and E_F becomes the same throughout at equilibrium, the conduction band edge E_C bends upward (Fig. 1.1(i)). If the band gap of the semiconductor is not changed, the valence band edge will also move up parallel to the conduction band edge E_C. Also, the electron affinity (χ_s) of the semiconductor is assumed to remain unchanged. Hence, the vacuum level should similarly bend upwards to maintain the value of χ_s. Thus, the vacuum level remains continuous across the transition region. Depending upon the work function of the metal and electron affinity of the semiconductor different situations may arise as shown in Fig. 1.1 (ii)

A dipole layer is built up at the interface due to the flow of the charge ,the size of which can be estimated by considering the screened coulomb potential of a point charge at a distance 'r'[6,7],

$$\phi(r) = (q/r)exp(-r/r_{TF}) \tag{1.1}$$

where q is the electronic charge and $r_{TF} = 0.5(n/a_o)^{-1/6}$ is the Thomas Fermi screening length; a_o is the Bohr radius and n is the electron density. With n$\sim$ $10^{22}cm^{-3}$(i.e., for metals), r_{TF} is ~ 0.55 $\AA$ and with n$\sim$ $10^{18}cm^{-3}$(e.g. ,for semiconductor) is $\sim 500\AA$. Thus a normal space charge layer (depletion or accumulation type) is

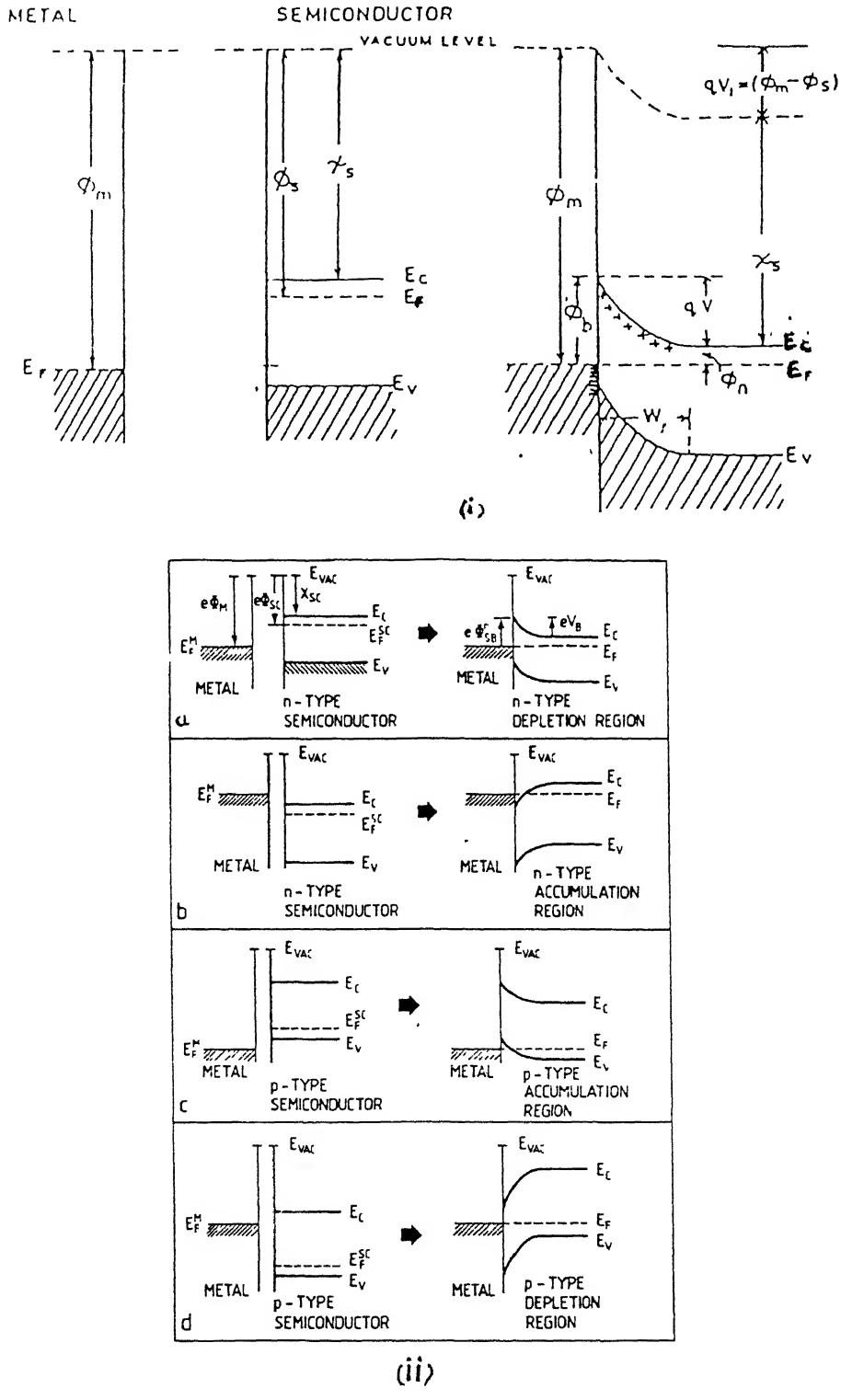

Figure 1.1: Schematic diagram of band bending before and after metal- semiconductor contact (a) High work function metal and n-type semiconductor ,i.e., $\phi_m > \phi_s$,(b) low work function metal and n-type semiconductor , (c) high work function metal and p-type semiconductor , (d) low work function metal and p-type semiconductor [6]

formed. The amount of band bending in the depletion region is correlated with the positive space charge of ionized donors via Poisson's equation

$$\frac{d^2V}{dz^2} = \frac{-\rho(z)}{\epsilon\epsilon_0}$$

where V is the potential, $\rho(z)$ is the space charge density at a distance z from the interface. The positive charge is balanced on the metal side by a corresponding excess electronic charge extending over a subatomic distance. The maximum band bending eV_b is just equal to the difference between two vacuum levels(see, e.g. Fig 1.1(i)).Thus,

$$eV_b = \phi_m - \phi_s \tag{1.2}$$

where V_b is the potential barrier encountered by an electron moving from the semiconductor to the metal.

The potential barrier $e\phi_b$which has to be overcome when an electron is excited from the metal into the conduction band of the semiconductor is given by

$$\phi_b = \phi_m - \chi \tag{1.3}$$

Using equation 1.1 and substituting $\chi = \phi_s - \phi_n$. we have

$$\phi_b = qV_b + \phi_n \tag{1.4}$$

Schottky assumed the semiconductor to be uniformly doped , giving a constant charge density in the depletion region. The electric field strength therefore rises linearly with distance from the edge of the space charge layer[4]. Mott assumed a thin layer devoid of charges sandwiched between a uniformly doped semiconductor and the metal. The electric field strength within the so called depletion region is constant[4]. The depletion region has few mobile carriers and hence has very high resistance . Consequently , a large part of the externally applied voltage drops across

the depletion region. If a negative voltage (V_f) is applied at the semiconductor , the depletion region width decreases and voltage across it falls from V_b to V_b-V_f.The electrons now see a reduced barrier and move from the semiconductor towards the metal causing a current flow . Since no voltage drop occurs within the metal , ϕ_b remains unaffected and there is no electron flow from metal to semiconductor . Thus MS junction exhibits rectifying properties.

The difficulties involved with this simple approach are obvious. Firstly, the barrier height in practise does not increase linearly with ϕ_m in accordance with equation (1.3) and (1.4). Secondly, the real work function is not a constant but depends on the surface orientation and gets strongly affected by types of rearrangement of surface atoms , e.g. , relaxations and reconstructions[6] . Here the nature of surface and interface comes into picture.

1.3 Surface and Interface states

The bulk crystal structure is broken at the surface so that the coordination of species becomes markedly different.For the topmost surface atoms the bonding partners on one side are missing in total .Therefore , their wave functions have less overlap with that of the neighbouring atoms.The splitting and shift of the atomic energy levels is thus smaller at the surface than in the bulk. According to Bardeen broken (or dangling) bonds at the semiconductor surface give rise to localised energy states called surface states. These states are distributed in the band gap and are characterized by a neutral level ϕ_o . That means when there is no band bending in the semiconductor, the surface states are occupied right upto ϕ_o making the surface neutral , i.e., a flat band condition (Fig.1.2)[4] . The states below ϕ_o are donor like while those above behave like acceptors . Depending upon the type of surface states and on the position of the Fermi level , the surface state may carry a charge , which is screened by an opposite charge inside the semiconductor.If an example of

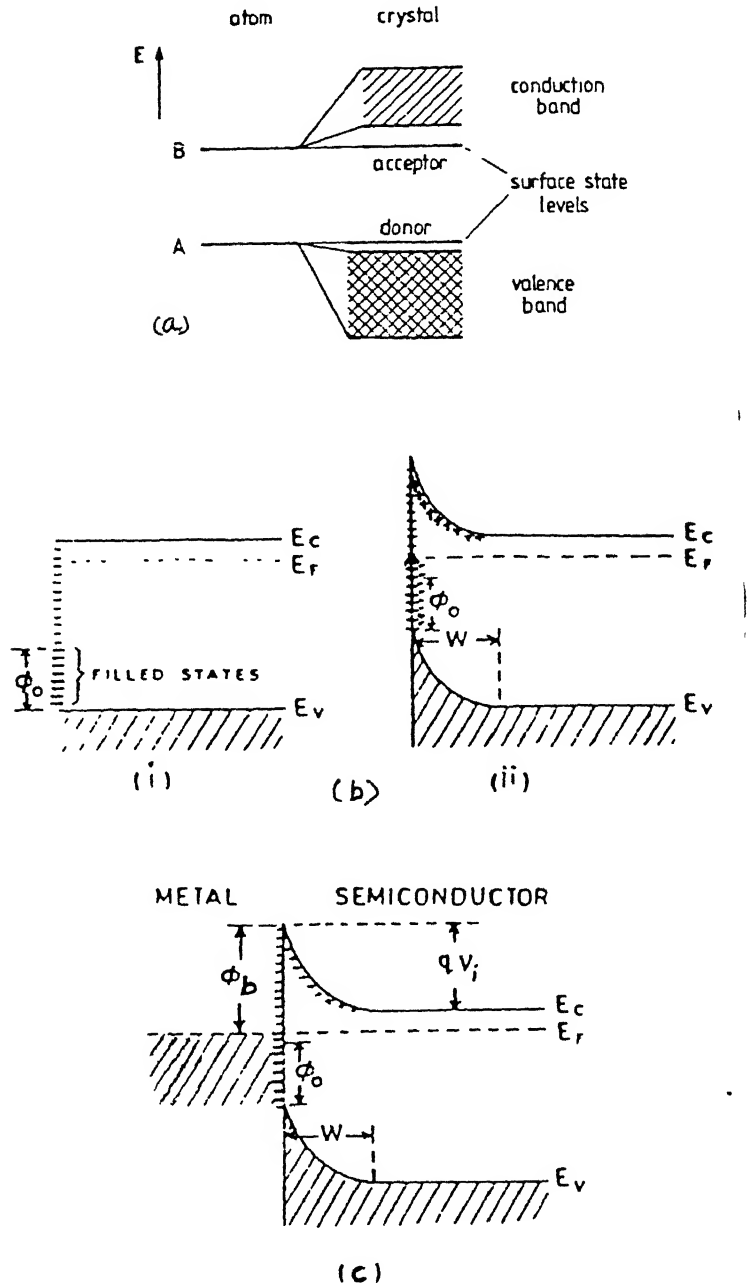

Figure 1.2: (a) Qualitaive explanation of the origin of surface states in the tight binding picture . Depending on their origin , these states have acceptor or donor like charging character (b) Electron energy band diagram of n-type semiconductor with surface states (i) under flat band ,(ii) in thermal equillibrium with thc bulk, and (c) in contact with metal [4,6]

a n-type semiconductor is taken , we have acceptor surface states ; their energetic positions being fixed with respect to E_c. Flat bands upto the surface would position the Fermi level far above the acceptor type surface states; filling them completely by electrons and building up an uncompensated charge density.This is energetically unfavourable and hence band bending is there at the clean surface even in the absence of metal contact[6] .

A different approach is via the mathematical treatment of Schokley[ ] . Here, a monoatomic linear chain terminated at one end is considered and the Schroedinger wave equation is solved for an electron under nearly free electron approximation. Possible solutions , with real electronic wave functions , are standing Bloch waves within the chain , matched to the exponentially decaying tails on the terminated side.Hence, the electronic energy levels are slightly modified from those of infinite bulk. Additional surface solutions become possible if complex wave vectors are allowed. The calculation then yields one single electronic surface state located in the gap of bulk states.Electrons in these states are localized within a couple of Angstroms of the surface plane.The results can be generalised to the 2D surface[6]

.

Numerous experiments on the wide variety of MS systems prepared under UHV conditions indicate that the deposition of metal films produce interface states which determine the position of the Fermi level at the contact[6] . According to Heine [ ] metal (Bloch) wavefunctions tail into the semiconductor in the energy range in which the conduction band of metal overlaps the forbidden gap of the semiconductor. Fig.1.3(b) represents the situation in greater detail. The breakdown of the periodcity at the interface introduces exponentially decaying interface states with imaginary wave vectors. which fills the energy gap of the semiconductor symmetrically with respect to the band edges E_c and E_v . In a simple 1D model their dispersion curve E-q (Fig. 1.3(a)) indicates the range of theoretically possible

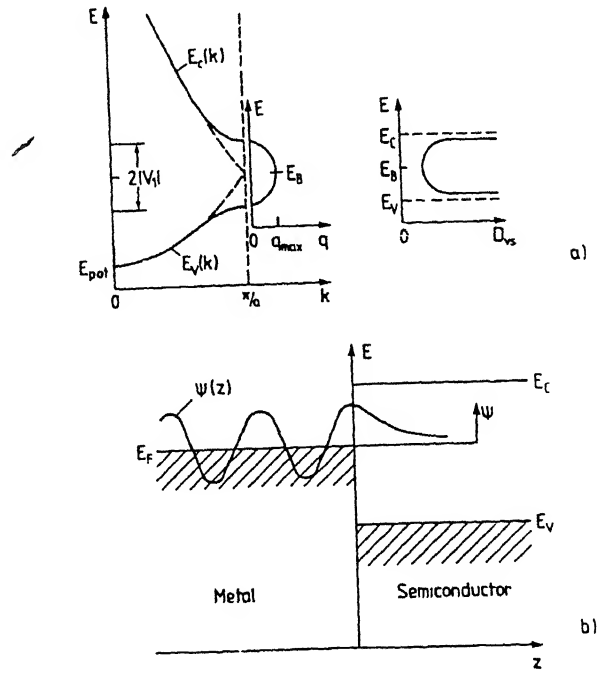

Figure 1.3: Origin of metal induced gap states at MS interface (a) Dispersion curve of a 1D model of semiconductor ; the real band structure with $E_c(k)$ and $E_v(k)$ as conduction and valence bands respectively. D_{vs} is density of the virtual states (b) Tailing of metal Bloch state into semiconductor

states known as "Virtual induced gap states"(VIGS). In the case of free surface , only a single energy level exists , but in the present case ,the Bloch states of metal conduction band have to match resulting in a broad continuum of states in the energy gap of the semiconductor.Or else, the continuum of metal states leaks into the VIGS which are themselves derived from the semiconductor band structure . Which of these states actually exist depends on the boundary conditions at the interface.

Fig.1.4 shows barrier heights as predicted by the Schottky ,Bardeen models together with experimental findings for various metal-silicon contacts. Accordingly , the experimental result lie in between the two extreme approaches namely Schottky with no interface states and the Bardeen with high density of interface states. If the density of surface states is high , the charge exchange takes largely between the metal and the surface states and the space in the semiconductor nearly remains

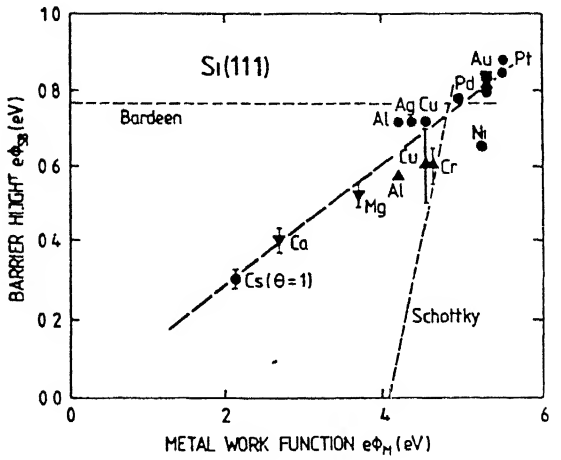

Figure 1.4: Barrier heights of Si-Schottky contacts versus metal work function. For comparison the predictions of the Schottky (no interface states) and the Bardeen (high density of interface states) model are given [6].

unchanged. As a result , barrier height becomes independent of the metal work function and is given by [4]

$$\phi_b = E_g - \phi_o \tag{1.5}$$

Here the barrier height is said to be pinned by surface states and equation(1.4) is known as the Bardeen limit. The assumptions of Bardeen are,of course, incorrect , since the surface states of the clean surface are strongly affected by metal deposition. Taking into account the interface states , the Schottky barrier diode can be described as follows(Fig.1.5):

When the metal comes into close contact with the semiconductor surface , they'll form chemical bonds . The distribution of intrinsic surface states of the clean semiconductor surface will be changed . Charge will flow from one side to other due to formation of bonds which is described by the formation of a dipole layer of atomic dimensions. The direction of the dipoles is determined by the difference between the work function and electron affinity. Formation of new interface states is expected in all the cases. In a more extensive band scheme of the MS contact ,

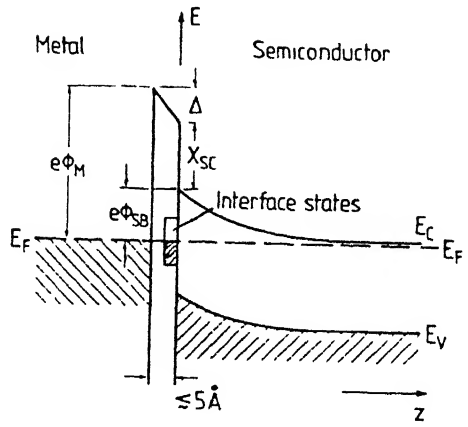

Figure 1.5: Band diagram of a metal-semiconductor junction in which the interface region (width ~5 Å) is taken into account explicitly

interface region could be included with its atomic dimensions. Using the metal work function(ϕ_m) and the electron affinity (χ_s)of the semiconductor , dipole energy (δ) can be associated to the interface layer . The total charge balance at the interface now includes the space charge in the semiconductor and the charges present in the metal and those located in the interface states. In thermal equillibrium , no net current flows . It is obvious that the band bending and in turn , the Schottky barrier height depends on the nature of the interface states.The origin and character of these states need to be further investigated for better understanding of the Schottky barrier formation.

1.4 Conduction Mechanisms

The various ways in which electrons can be transported across the MS junction under forward bias is shown schematically in Fig.1.6 for an n-type semiconductor. The inverse processes occur under the reverse bias condition . The mechanisms involve: (a) emission of electrons from the semiconductor over the top of the barrier into the metal (b) quantum mechanical tunneling through the barrier (c) recom-

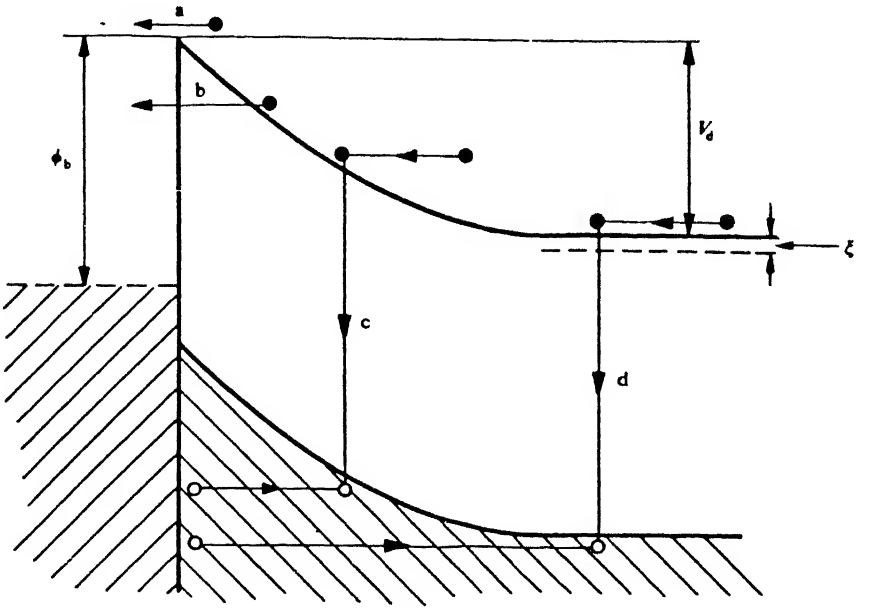

Figure 1.6: Transport processes in a forward-biased Schottky contact [4].

bination in the space charge region (d) recombination in the neutral region(hole injection)[4]

1.4.1 Thermionic emission-diffusion Mechanism

The motion of an electron crossing over the barrier from the semiconductor into the metal , moving through the high field depletion region, is governed by the drift and diffusion processes[ ]. Density of the available states, in fact controls the jumping (or emission) of electron into the metal. The two processes , the emission over the barrier and the drift and diffusion in the depletion region are effectively in series and the one which offers the higher resistance determines the current. In Bethe's TE theory [7] , it is assumed that the barrier height is much larger than kT and the effect of drift and diffusion in the depletion region is negligible. Hence , the current flow depends solely on barrier height. Schottky in his diffusion theory had also included the effect of electron collisions within the depletion region and assumed the carrier concentration at any distance to be unaffected by current

flow.Both the approaches led to the similar current expressions. According to the synthesis of the two theories proposed by Crowell and Sze [ ] the net current due to flow of electrons from semiconductor to metal by overcoming the potential barrier of height ϕ_b at a forward bias V is given by[4,7]

$$I = A_d A^{**} T^2 exp(\frac{-q\phi_b}{kT})[exp(\frac{qV}{kT}) - 1] \tag{1.6}$$

where A^{**} is the effective Richardson constant, A_d is the diode area , T is the temperature in Kelvin , k is the Boltzmann constant and q is the electronic charge.For free electrons Richardson constant is 1.12 x 10^6 $Am^{-2}K^{-2}$. However , the barrier height is known to increase with forward bias. If the variation is assumed to be linear , we can write [7]

$$\phi_b(V) = \phi_{bo} + \gamma V \tag{1.7}$$

where ϕ_{bo} is the barrier height at zero bias and γ $(= \frac{\delta\phi_b}{\delta V})$ is positive. Substituting the value of $\phi_b(V)$ into eqn (1.6) , we get

$$I = I_s exp(\frac{qV}{\eta kT})[1 - exp(\frac{-qV}{kT})] \tag{1.8}$$

where

$$I_s = A_d A^{**} T^2 exp(\frac{-q\phi_{bo}}{kT}) \tag{1.9}$$

and

$$\frac{1}{\eta} = 1 - \gamma$$

The parameter η is called the ideality factor and usually has a value greater than unity. Further , the presence of a series resistance(R_s) causes significant voltage drop at large forward currents.As a consequence , the current equation (1.8) gets modified to

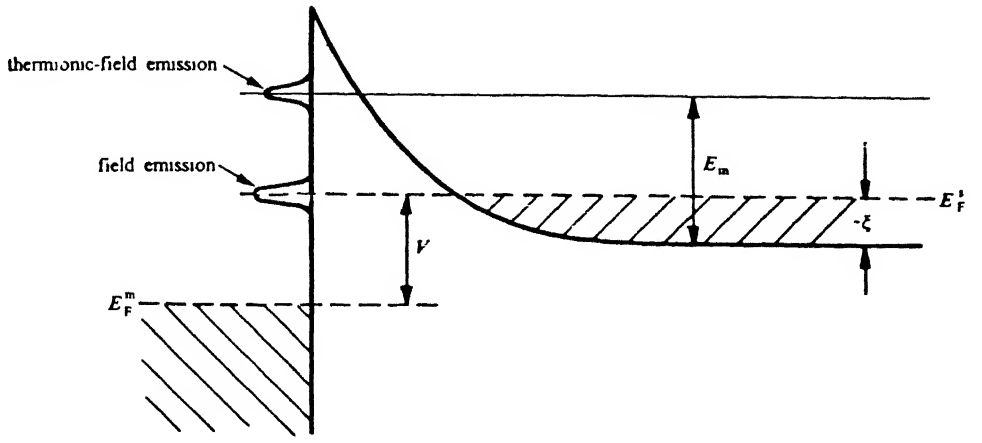

Figure 1.7: Field and thermionic-field emission under forward bias [7].

$$I = I_s exp(\frac{q(V - IR_s)}{\eta kT})[1 - exp(\frac{-q(V - IR_s)}{kT})] \quad . \quad (1.10)$$

Also, the ln(I) vs V plot begins to deviate from linearity and exhibits saturation.

1.4.2 Tunneling through the Barrier

This mechanism prevails when the semiconductor is heavily doped such that the Fermi level lies above the bottom of the conduction band and depletion width is very small. It may be possible for electrons with energies below the top of barrier to penetrate by the well known quantum-mechanical tunneling. In the case of degenerate (heavily doped) semiconductor at low temperatures , the current in forward direction arises from the tunneling of electrons with energies close to Fermi energy in the semiconductor . This process is known as field emission (FE) . At raised temperatures , electrons excited to higher energies have higher tunneling probability as they experience thinner and lower barrier . This is known as thermionic field emission (TFE) [4] (Fig.1.7). If the temperature is still raised further , a point is reached in which virtually all the electrons have enough energy to go over the top

of barrier; it is pure thermionic emission with negligible tunneling.The tunneling current through the barrier is of the form [4, 12, 13]

$$I_t = I_{to} exp(\frac{q(V - IR_s)}{E_o})[1 - exp(\frac{-q(V - IR_s)}{kT})] \tag{1.11}$$

where

$$E_o = E_{oo} coth(\frac{E_{oo}}{kT}) \tag{1.12}$$

and I_{to} is the saturation tunneling current. E_{oo} is defined as

$$E_{oo} = \frac{h}{4\pi}\sqrt{\frac{N_d}{m_e{}^* \epsilon_s}} = 18.5X10^{-15}\sqrt{\frac{N_d}{m_r \epsilon_r}}\ eV \tag{1.13}$$

where $m_e{}^*$(=$m_r m_o$)is the effective mass of the electron and ϵ_s (=$\epsilon_r \epsilon_o$) is the permittivity of the semiconductor, m_o is the electron rest mass and N_d is the donor concentration in m^{-3}. The process is FE when E_{oo}>>kT and is TFE at $E_{oo} \approx$ kT . TFE also causes a reduction in barrier height by [4]

$$\Delta\phi = (\frac{3}{2})^{\frac{2}{3}} E_{oo}{}^{\frac{2}{3}} V_d{}^{\frac{1}{3}} \tag{1.14}$$

where V_d stands for the voltage corresponding to the band bending. Eqn (1.11) suggests that $\ln I_t$ vs V plot should yield a straight line with slope giving E_o and intercept at zero bias the saturation current I_{to}.

1.4.3 Carrier Generation and Recombination

At zero bias there exists a thermal equillibrium , as the rate of electron-hole pair generation in the depletion region is balanced by the rate of recombination. With the application of bias, however , np product departs from $n_i{}^2$ and a net generation or recombination of carriers occur depending upon the polarity. In case of a Schottky diode made on n-type silicon ,when the substrate is forward , biased electrons are

injected into the depletion region from the neutral bulk semiconductor and the holes are swept away from the metal . These additional electron-hole pairs combine in the depletion region to give a forward combination current . The recombination current can then be described by [4]

$$I_r = I_{ro}[exp(\frac{qV}{2kT}) - 1] \tag{1.15}$$

$$with \;\; I_{ro} = \frac{qn_i A_d w}{2\tau} \tag{1.16}$$

$$and \;\; n_i = \sqrt{N_c N_v} exp(\frac{-E_g}{2kT}) \tag{1.17}$$

Here w is the width of the depletion region , τ is the effective carrier lifetime within the depletion region , n_i is the intrinsic carrier concentration , E_g is the energy band gap and N_c and N_v are the effective conduction and valence band density of states, respectively.

1.4.4 Minority Carrier Injection

Under the low bias conditions , the Schottky barrier diode is a majority carrier device. But, at large forward bias , minority carrier current contribution increases and becomes more than the diffusion current. The electrons flow from the semiconductor into the metal under the forward bias and some of the holes are swept into the neutral region . The current I_p caused by hole injection from metal into the neutral region of n-type semiconductor of donor concentration N_d is given by [14]

$$I_p = \frac{qA_d D_p {n_i}^2}{N_d L_p}[exp(\frac{qV}{kT}) - 1] \tag{1.18}$$

where D_p is the hole diffusion constant , $L_p = \sqrt{D_p \tau_p}$ is the hole diffusion length and τ_p represents the hole lifetime in the neutral region.

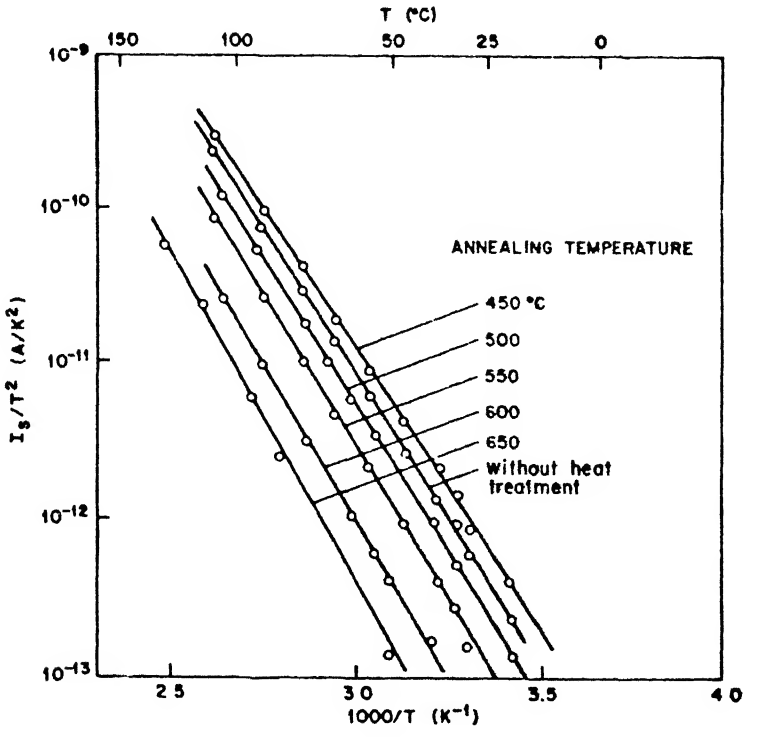

Figure 1.8: Activation energy plots for determination of barrier height [7]

1.5 Methods of Barrier Height Measurement

In general , the barrier height is measured either using the current-voltage or internal photoemission or the capacitance-voltage characteristics. On the basis of thermionic emission-diffusion (TED) mechanism , the current through the Schottky barrier diode at a forward bias V is given by eqn (1.6). The plot of ln(I) vs V is linear upto a point , for the forward bias V in excess of 3kT/q [4] . Afterwards the plot deviates showing saturation due to the series resistance term. In the plot of ln(I) vs V, the straight line portion is extrapolated to zero bias , so that the intercept at the ordinate is ln(I_s). By substituting the values of effective Richardson constant A** , saturation current I_s in eqn (1.5) , zero bias barrier height ϕ_{bo} can be determined at a temperature T for a given diode area A_d.The value of ϕ_{bo} is not very sesitive to the choice of A** since at room temperature a 100% increase in A** causes an increase of only 0.018Vin ϕ_{bo} [7].

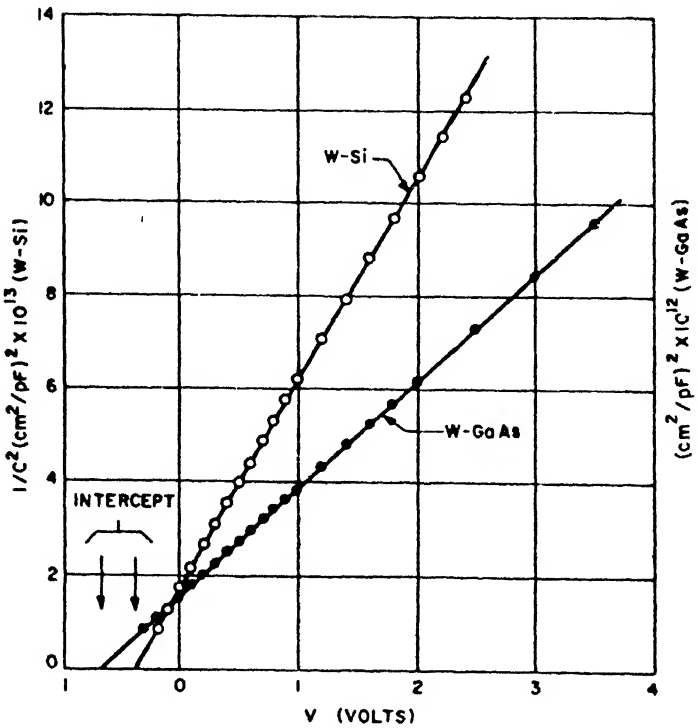

Figure 1.9: $1/C^2$ versus applied voltage for determination of barrier height [7]

Also , the activation energy (or the Arrhenius) plot i.e. ln (I_s/T^2) vs $1/T$ plot (Fig.1.8) can be made using saturation current data at various temperatures. ϕ_{bo} can be obtained from the slope of the best fit line [4]. Here the intercept at the ordinate is ln(A** A_d) where A_d is the electrically active area. The main advantage in this approach is that the value of A_d is not at all required for the evaluation of ϕ_{bo} .

Second method of determining the barrier height is by measurement of the capacitance of the Schottky diode as a function of reverse d.c. bias(V_R)(Fig.1.9). The charges of opposite signs are induced on the metal surface and in the depletion region of the semiconductor when a small a.c. voltage of few mV is superimposed on a d.c. bias. The relationship between the capacitance (C) and reverse bias V_R is given by[1]

$$C = A_d \sqrt{\frac{\epsilon_s q N_d}{2(\phi_b - \phi_n - V_R - \frac{kT}{q})}} \tag{1.19}$$

where ϵ_s is the permittivity of the semiconductor, N_d is the dopant concentration , ϕ_n is the distance of the Fermi level from the bottom of the conduction band and other symbols have their usual meanings. Thus , if $1/C^2$ is plotted against V_R , a straight line with a slope of $(2/A_d{}^2 \epsilon_s q N_d)$ is obtained having an intercept on the voltage axis V_{RO} at which $1/C^2$ is zero.The value of barrier height ϕ_b can be than easily obtained as [4]

$$\phi_b = V_{RO} + \phi_n + \frac{kT}{q} \tag{1.20}$$

and ϕ_n, the depth of Fermi level below the conduction band , can be computed from the doping concentration N_d. N_d can be evaluated from the slope of $1/C^2$ vs V_R plot too.

1.6 Importance and Applications

All the practical applications exploit the inherent high speed advantages of majority carrier conduction in Schottky diodes.The most important commercial application of Schottky diodes is in bipolar integerated circuits as clamps and to a lesser extent as load resistor substitutes ,diode couplers and level shifters.They are also used as discrete microwave transistors , optical and nuclear particle detectors, etc.The Schottky diode is preferred over the pn junction diode because of high forward conductance per unit area , large reverse impedance , fast switching speed about 1ns , compact size ,and relatively easy fabrication technology at quite low temperatures. Metal-semiconductor rectifiers are relatively immune to the speed limitation associated with the minority carrier storage in p-n junction devices [15-17] . However, the reverse current in a Schottky barrier is quite large,

and is disadvantageous . Also , it is a surface device and hence sensitive to surface contamination and perimeter effects.

1.7 Objective of the present work

Extensive studies have been undertaken on different aspects of Schottky barrier diodes with the view to understand their characterstics better and find newer applications [3,4,18-21]. The most important aspect of metal-semiconductor contacts is the process which determines the flow of charges over the barrier from the semiconductor to the metal and vice- versa. Detailed knowledge of the conduction process involved is needed to extract the values of the barrier parameters.The I-V characteristics of Schottky diodes formed by depositing various metals such as Ir, Pt, Cr, Er, W ,Cu, and Ti on silicon have been studied in detail [22-32].

The fewer reports are available for Pd/Si Schottky diodes in particular and contain limited information on the conduction mechanisms ,e.g., Chin et. al. [33] studied Pd_2Si/Si Schottky barrier diodes on n-type silicon at 300K and on p-type silicon at 84 K . Werner and Guttler [34] reported some data on Pd_2Si Schottky barrier diodes while describing the temperature dependence of barrier heights for various metals on n-type silicon. Chand and Kumar [35-39] have recently studied Pd_2Si/n-Si contacts over a wide temperature range and interpreted the results on the basis of thermionic-emission-diffusion mechanism, assuming the presence of a Gaussian distribution of barrier heights at the interface.

The current-voltage (I-V) characteristics of Schottky barriers measured at room temperature do not give adequate information about the conduction process and the nature of the barrier formed at the metal-semiconductor interface. Details of many possible effects that cause non-ideality in the diode I-V characteristics , and , in general , reduce the barrier height cannot be ascertained. The temperature dependence of the I-V measurements gives a better picture. Also, Schottky barriers

in devices operating in space and in some other applications are subjected to wide range of temperatures. So, information about their electrical characteristics over wide temperature range helps in understanding the actual working of these devices as well.

An attempt has been made here to fabricate Pd/n-Si Schottky contacts and study their I-V characteristics in a wide temperature range (80K-300K). Since, fabrication involves deposition of palladium metal film and subsequent annealing , identification and growth of resulting phase(s) of silicide have also been explored using X-ray diffraction and reflectance measurements in UV-Visible range (200-900nm). In addition , simulation of (1) current-voltage (I-V) characteristics have been carried out for various mechanisms with a view to exmine their relative contributions and dominance , and, (2) apparent barrier height (BH) as a function of temperature . For the later case , barrier inhomogenities are believed to be present at the contact and described by a Gaussian distribution of barrier heights with a mean (ϕ_b^-) and standard deviation (σ_o). In this, uniqueness lies in considering the linear temperature dependence of the mean and variance (σ_o^2). The purpose is to understand the effect of various parameters in detail.

Chapter 2
Experimental

2.1 Fabrication of Schottky diodes

The Schottky diodes were fabricated upon n-type (phosphorus doped) silicon wafers of (111) orientation . The n/n^+ silicon wafers had a 8-9 μm thick epitaxial n layer of resistivity $\sim$2.6 ohm-cm($N_d = 3.9X10^{15}$ cm^{-3}) over the heavily doped n^+ region. The wafers were first degreased with soap solution and then were thoroughly cleaned with organic solvents, viz, trichloroethylene , acetone and methanol in succession in an ultrasonic cleaner and rinsed in deionised water and dried.

The back contact (ohmic) was made by depositing a layer of aluminium on the heavily doped n^+ side of the silicon wafer after usual cleaning and etching in dilute HF ($HF:H_2O$=1:10) followed by washing in deionised water.A$\sim$ 200 nm thick aluminium deposition was carried out in a HHV coating unit model 12A 4D under vacuum $\sim 10^{-5}$ mbar, at 450^o C for 30 minutes after introducing in a quartz tube , placed in a tubular furnace and connected to a pumping system model HHV VS114D. The silicon wafers were cleaned again from the epitaxial n or p layer (i.e. front) side in trichloroetylene ,acetone and methanol and then etched in the dilute hydrofluoric acid ($HF:H_2O$=1:10) and rinsed in deionised water for removal of silicon dioxide layer that usually forms on the silicon wafer during exposure to the ambient, aluminium deposition step and annealing. The back contact of the aluminium was protected from HF by laying a wax coating. Palladium film($\sim$80 nm thick) was deposited by employing an electron beam evaporation source in a HHV coating unit model 12A 4D-SC on to the cleaned epitaxial n-layer through circular holes of diameter 1 mm in a stainless steel mask. Subsequently, the samples

were taken out of the work chamber and put inside a quartz tube as before and annealed in vacuum of the order of~ 3-5 x 10^{-6}mbar at 300°C, 400°C, 450°C, 500°C for various durations to form palladium silicide. The silicon wafers were finaly cut into small pieces such that each contained a palladium silicide dot and mounted on to a TO5 header through silver epoxy. The contact to the top metal dot was established through a thin gold wire.

2.2 Setup for I-V-T measurements

An automated setup shown in figure 2.1 was used to record the I-V characterstics of Schottky diodes was over a wide temperature range (80K-300K). The bias was applied from a Keithley programable voltage source model 230 in steps of 5-10mV and the current through the diode was recorded with Keithley picoamèter model 485 through a computer controlled system. To ensure steady state conditions, a delay of few seconds was observed between subsequent measuring steps. For recording the tempreture dependence of the I-V characterstics in the range 80K-300K a CTI-cryotronics close cycle helium refrigerator model 22C equipped with a Lake Shore temprature controller model 330 was employed.

2.3 Phase identification microstructure and reflectance measurements

For identification of the phase(s) formed and studying the growth kinetics of silicide, palladium film was deposited on a bare silicon wafer after usual cleaning and etching in hydrofluoric acid exactly in manner described in section 2.1, but without mask. Samples were annealed at 200°C, 400°C, 450°C and 500°C for various durations in vacuum~ 3-5x10^{-6}mbar. Rich Siefert ISO-Debyeflex 2002 X-ray diffractometer with CuKα radiation (λ=1.5418Å) was employed to record the diffraction patterns. The calibration of the system was carried out with a standard

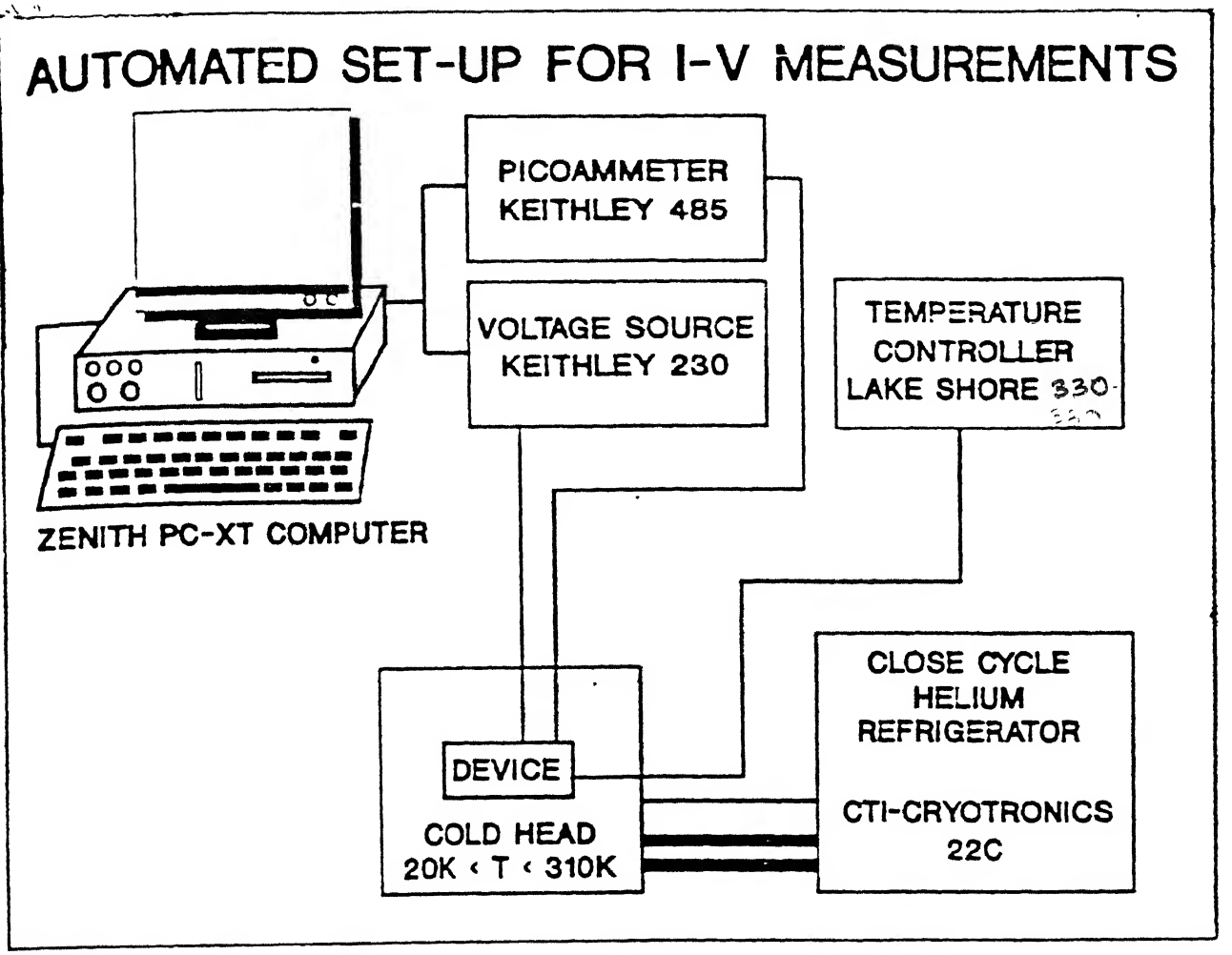

Figure 2.1: Block diagram of automated set-up for I-V measurements of Schottky diode over a wide temperature range.

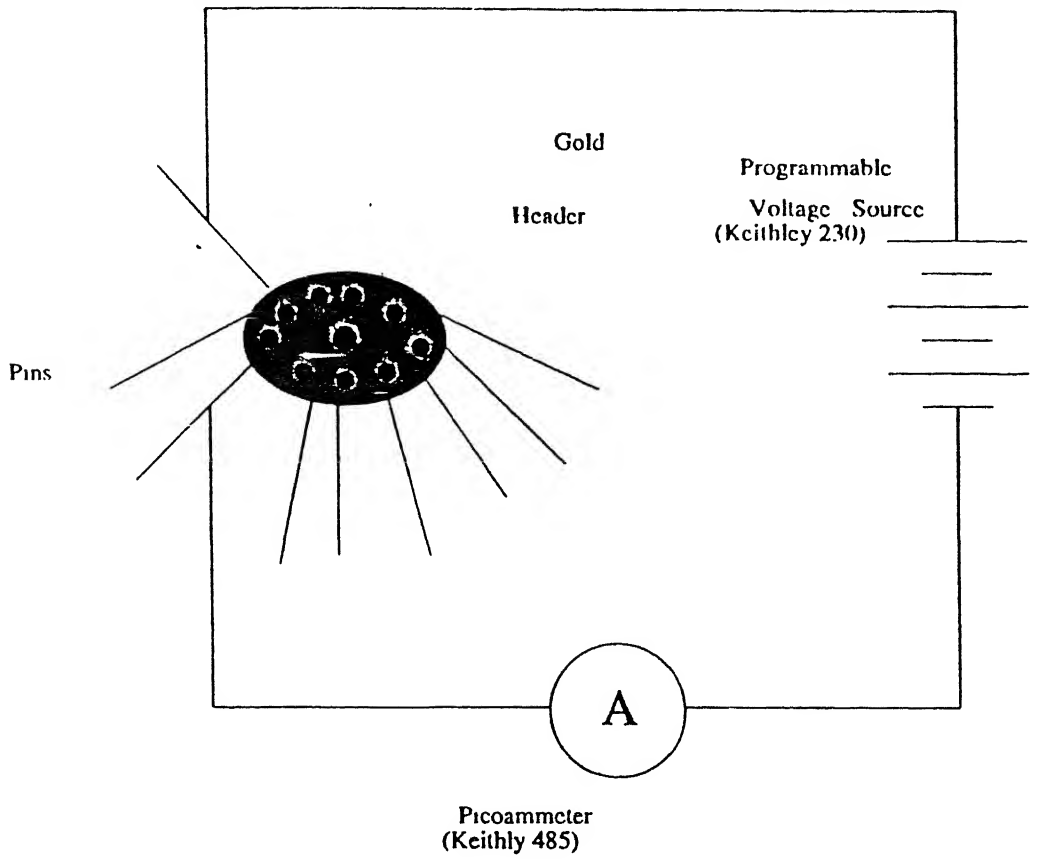

Figure 2.2: The circuit diagram for I-V measurements of a Schottky diode.

silicon sample. The observed X-ray diffraction peaks were indexed by determining the interplanar spacings (d) corresponding to various planes using the well known Bragg's law [40]2d sin $\theta = \lambda$, θ being the peak angle. The phase(s) identification was carried out by comparing the results with the standard data available in the powder diffraction files[41].

The microstructure of the samples annealed at various temperatures for different lengths of time was examined in scanning electron microscope JEOL JSM 840A in the secondary electron(SE) mode. Also, reflectance measurments at near normal incidence(by employing a 5° spacer) were carried out for the annealed samples in the wavelength range 200-900nm using a Hitachi UV 150-20 spectrophotometer equipped with a 60 ϕ integrating sphere.

Chapter 3
Results and Discussions

3.1 Forward I-V characteristics

The forward I-V characteristics of Pd_2Si Schottky diodes fabricated on n-type Si (111) as described in section 2.2 and annealed at 450°C for 45 min are shown in figure (3.1) at various temperatures in the range 80K-300K. Clearly, they are linear over several order of current. Further, they progressively become straight over a wide current range with decrease in temperature. Such an observation suggests the dominance of the thermionic emission-diffusion mechanism for current transport . A program in Basic is used to fit the experimental I-V data in the thermionic emission-diffusion current equation (1.10). It involves iteration method and takes I_s, η, and R_s as adjustable parameters.

3.1.1 Zero bias barrier height , ideality factor and series resistance

The zero bias barrier height (ϕ_{bo}) can now be evaluated from the I_s data by substituting the values of the effective Richardson constant A^{**}, diode area A_d, and temperature T. Thus ,ϕ_{bo} is found at each temperature from equation (1.9). Figure (3.2) shows the zero bias barrier height as a function of temperature. It clearly depicts that ϕ_{bo} decreases with fall in temperature steadily in the begining but quite rapidly below 120K.The variation of ideality factor and series resistance with the temperature are shown in figure (3.3) and (3.4) respectively . The ideality factor increases rather slowly with decrease in temperature but quite significantly at lower temperatures.There is a rapid increase of series resistance with fall in temperature

below 200K which is beleived to be due to factors responsible for increase in η and /or lack of free charge carriers at lower temperatures[22].

3.1.2 Activation Energy Plot

Equation (1.9) can be rewritten as

$$ln\frac{I_s}{T^2} = ln(A_d A^{**}) - \frac{q\phi_{bo}}{kT} \tag{3.1}$$

Therefore, the $\ln(I_s/T^2)$ vs $1/T$ (i.e. activation energy or Arrhenius) plot should exhibit a straight line with slope giving the zero bias barrier height (ϕ_{bo}) and intercept at the ordinate determining the Richardson constant (A^{**}) itself for the known diode area A_d. This method gives a single value of barrier height. The experimental results , however correspond to the $\ln(I_s/T^2)$ vs $1/T$ plot , shown in figure (3.5). The data fits to a straight line only at high temperatures , i.e. , above 180K. The slope of the curve is infact varying continuously.

3.2 Concept of Barrier Inhomogenities

According to Chand and Kumar [36-38] an abnormal decrease of barrier height (BH) and increase of the ideality factor (η) with the decrease in temperature cannot be explained adequately by incorporating interface states or interfacial oxide layer, tunneling , image force lowering and / or generation - recombination effects. A way to explain the abnormal behaviour of barrier height and ideality factor is to assume the existence of barrier inhomogenities and describe them with some suitable distribution function. Numerous evidences have since been reported for the existence of barrier height inhomogenities[42-44]. Inhomogenities may be due to variation in thickness and composition of the silicide layer, nonuniformity of the interfacial charges and locally defective hot regions[23].

Various types of distribution functions have been proposed to describe inhomogenities, e.g., a Gaussiah or a log normal. One can assume a Gaussian

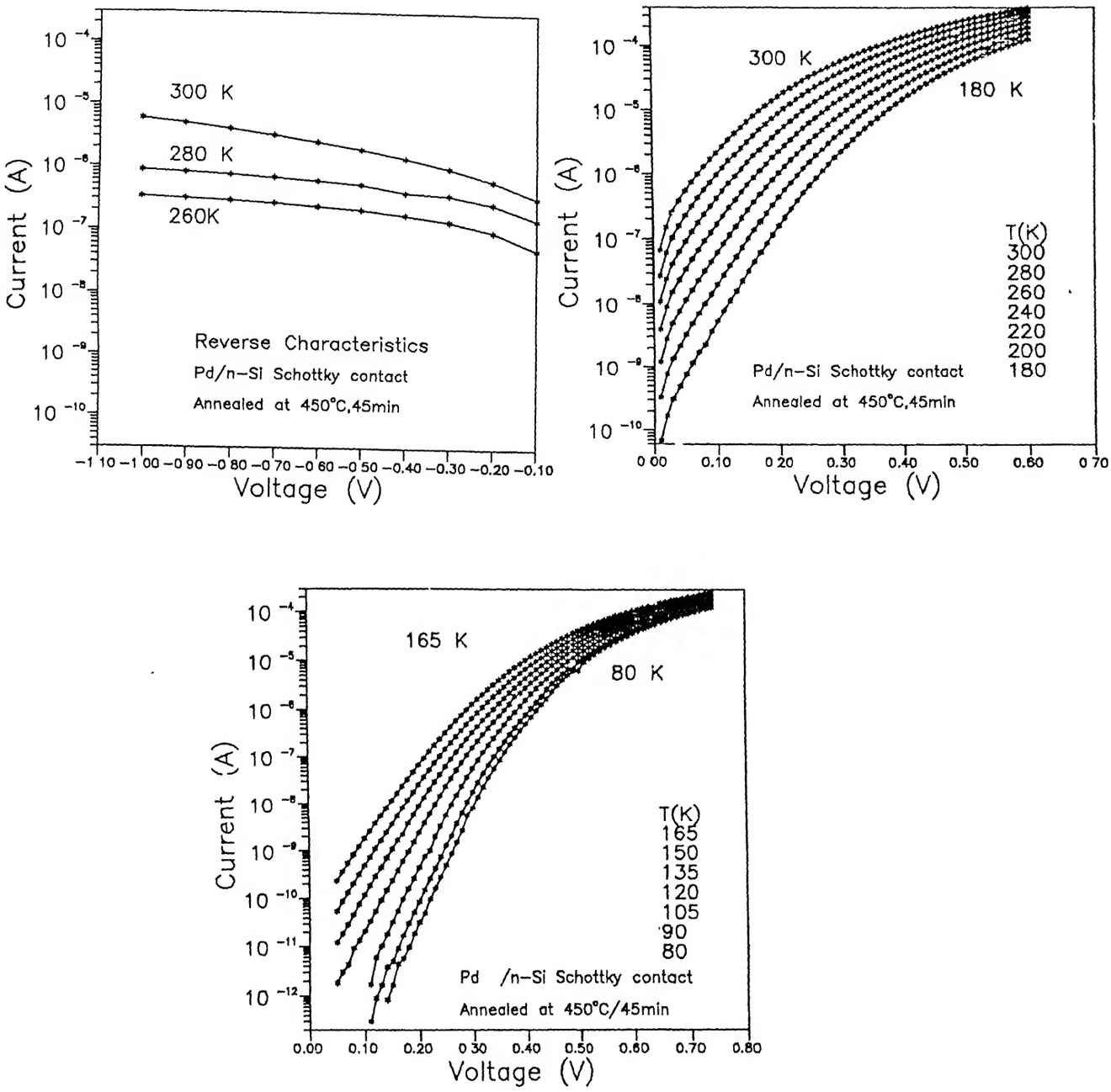

Figure 3.1: Current - voltage characteristics of Pd/n-Si Schottky contacts in the temperature range (a) 300K-180K (b) 165K-80K

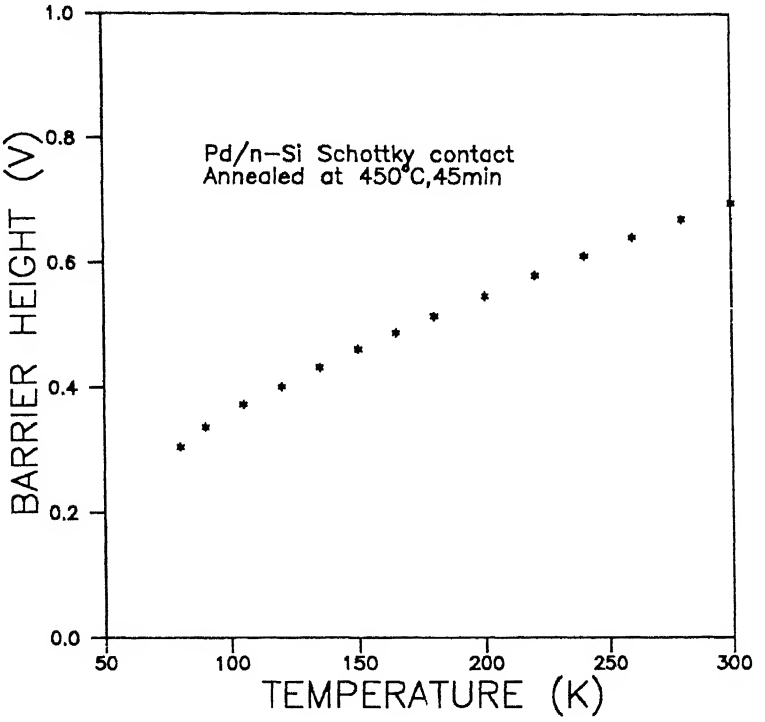

Figure 3.2: Variation of the zero bias barrier height ($\bar{\phi}_{bo}$) with temperature ,in the range 80K-300K

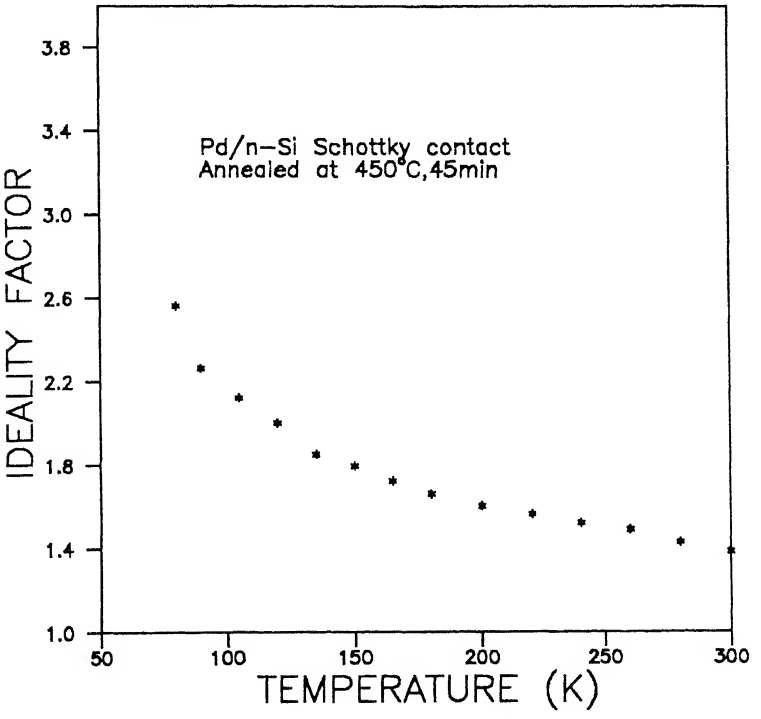

Figure 3.3: Temperature dependence of Ideality factor for Pd/n-Si Schottky contacts ,in the range 80K-300K. Notice the sharp increase in η at low temperatures.

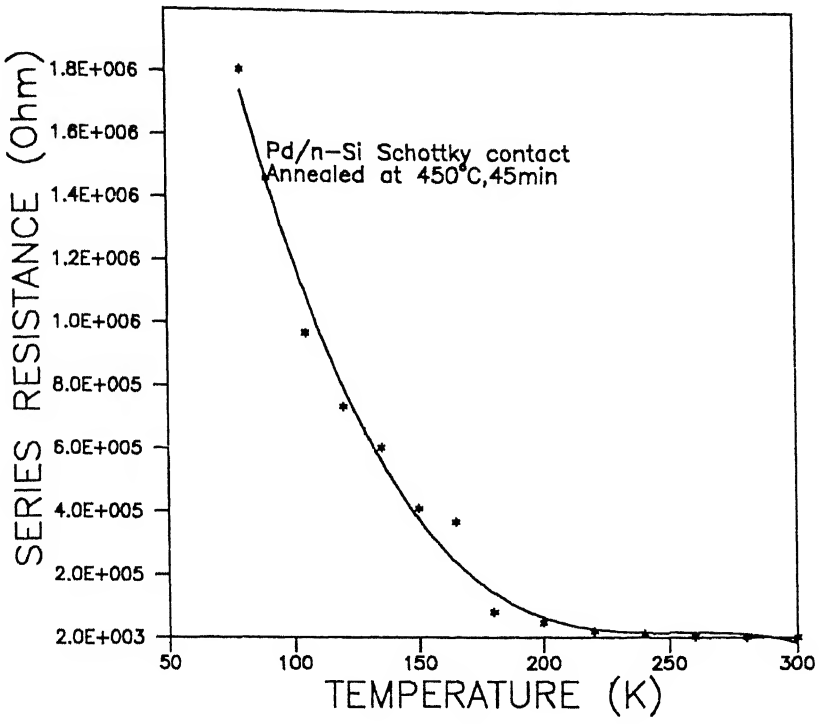

Figure 3.4: Temperature dependence of series resistance (R_s) for Pd/n-Si Schottky contacts ,in the range 80K-300K. Notice the sharp increase in R_s at low temperatures.

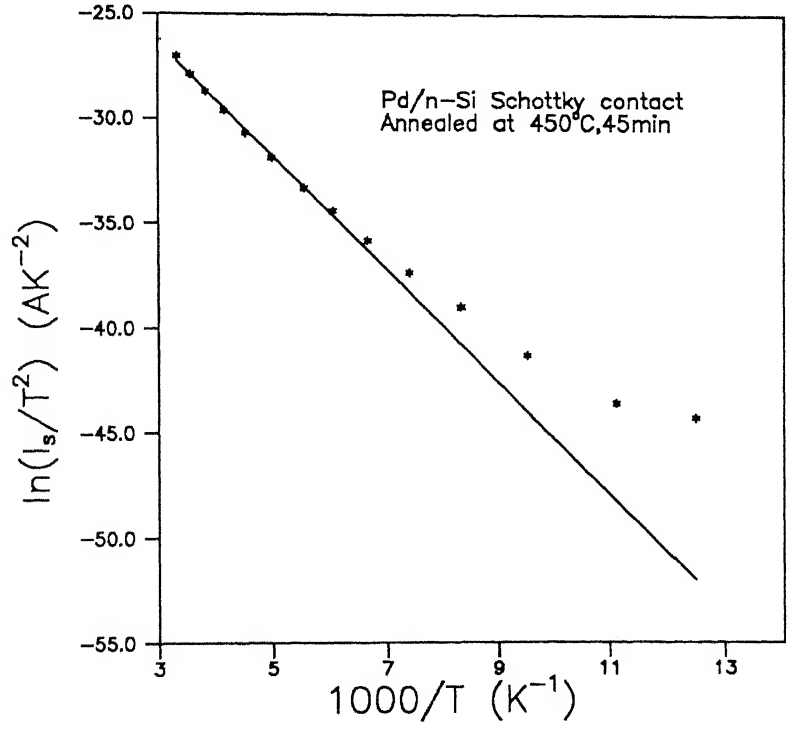

Figure 3.5: The $\ln(I_s/T^2)$ vs 1000/T plots of Pd/n-Si Schottky contacts with best fit straight line ,in the range 80K-300K. It shows non-linearity below 165K

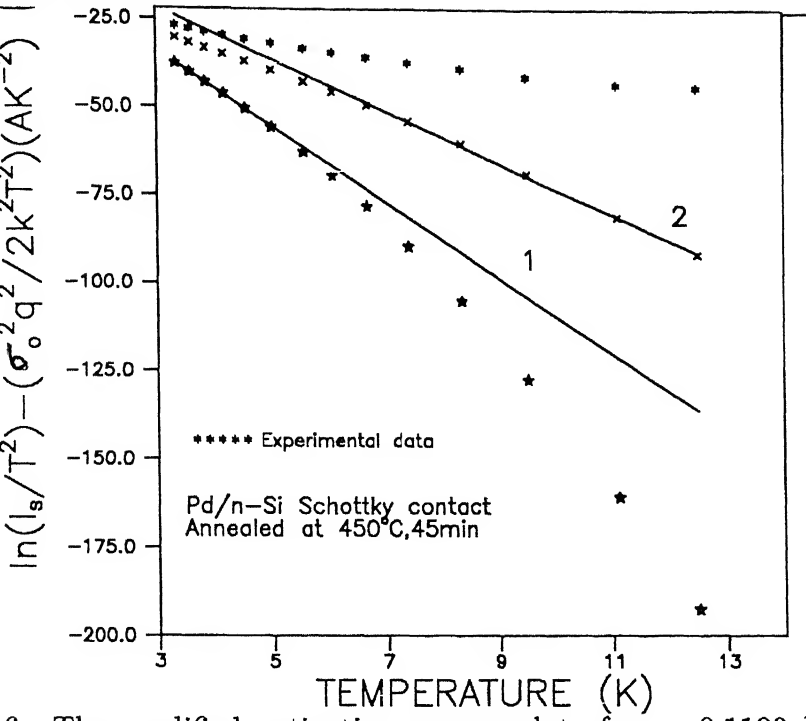

Figure 3.6: The modified activation energy plots for σ_o 0.1109 V and 0.063 V , together with the experimental data. The straight lines 1 and 2 indicate best fitting of data in temperature ranges 165-300K and 80-150K.

distribution of barrier heights with a mean value of $\bar{\phi}_b$ and standard deviation σ , having the form[23,45,46]

$$\rho(\phi_b) = \frac{1}{\sigma\sqrt{2\pi}} exp(-\frac{(\phi_b - \bar{\phi}_b)^2}{2\sigma^2}) \tag{3.2}$$

where preexponential term is the normalisation constant . The total current across the Schottky contact at a forward bias is then given by [47]

$$I(V) = \int_{-\infty}^{\infty} I(\phi_b, V)\rho(\phi_b)d\phi_b \tag{3.3}$$

where I(ϕ_b , V) is the current for an elementary diode having barrier height ϕ_b at bias V and is given by equation (1.10) in case of thermionic emission-diffusion process. Substituting I(ϕ_b , V) and $\rho(\phi_b)$ from equations (1.10) and (3.2) in (3.3) and performing the integration from $-\infty$ to ∞ one gets

$$I(V) = A_d A^{**} T^2 exp(-\frac{q}{kT}(\bar{\phi}_{bo} - \frac{\sigma^2 q}{2kT}))[exp(\frac{q(V - IR_s)}{kT}) - 1] \tag{3.4}$$

The barrier is known to depend on the electric field and hence on the applied bias [4]. Now , since barrier heights are represented by a Gaussian distribution, the entire profile should be affected by the applied bias. Hence considering the linear bias dependence of the distribution parameter, we have

$$\bar{\phi_b} = \bar{\phi_{bo}} + \gamma V \quad and \quad \sigma = \sigma_o + \xi V \tag{3.5}$$

where γ and ξ are positive derivatives , and $\bar{\phi_{bo}}$ and σ_o are mean barrier height and standard deviation at zero bias, respectively. Making these substitutions and neglecting the term involving $\xi^2 V^2$, equation (3.4) gets modified to

$$I(V) = I_s exp(\frac{q(V - IR_s)}{\eta_{ap} kT})[1 - exp(-\frac{q(V - IR_s)}{kT})] \tag{3.6}$$

with

$$I_s = A_d A^{**} T^2 exp(-\frac{q\phi_{ap}}{kT})$$

Here I_s is the observed saturation current , ϕ_{ap} and η_{ap} are the apparent barrier height and ideality factor respectively.ϕ_{ap} and η_{ap} are given by

$$\phi_{ap} = \bar{\phi_{bo}} - \frac{\sigma^2 q}{2kT} \quad and \quad \frac{1}{\eta_{ap}} = (1 - \gamma) + \frac{\sigma_o q \xi}{kT} \tag{3.7}$$

It is clear that ϕ_{ap} depends upon the distribution parameters (i.e. mean $\bar{\phi_{bo}}$ and standard deviation σ_o) and temperature T. Obviously, decrease in the barrier height is caused by mere existence of distribution and its effect becomes more and more pronounced at low temperatures. On the other hand, η_{ap} is a function of rate of change of both the mean $\bar{\phi_{bo}}$ and the standard deviation $\sigma_o$with the bias besides σ_o itself.

3.3 Interpretation of the Experimental Data

The diode parameters derived from the fitting of the experimental data in equation (3.6) can therefore be interpreted using equation (3.7) and (3.8) . Thus

the ϕ_{ap} vs 1/T plot should be a straight line giving $\bar{\phi}_{bo}$ and σ_o from the intercept at the ordinate and the slope respectively. The I-V data however, reveal , two straight lines in ϕ_{ap} vs 1/T plot giving two values of $\bar{\phi}_{bo}$ (0.93V and 0.63V) and σ_o (0.118 and 0.067V). Such an observation is , in fact attributed to the presence of two Gaussian distributions of barrier height at the interface and discussed in length later in section 3.4

Also combining equations (3.6) and (3.7) one obtains

$$ln(\frac{I_s}{T^2}) - \frac{q^2\sigma_o^2}{2k^2T^2} = ln(A_dA^{**}) - \frac{q\bar{\phi}_{bo}}{kT} \tag{3.8}$$

The nonlinearity in the activation energy plot can now be understood on the basis of equation (3.8). The factor $\ln(\frac{I_s}{T^2}) - \frac{q^2\sigma_o^2}{2k^2T^2}$ is calculated to modify the experimental data and plotted as a function of 1/T to obtain a straight line corresponding to a single activation energy around $\bar{\phi}_{bo}$ accurately. The intercept of the straight line at the ordinate gives the Richardson constant itself. Figure (3.6) shows the modified activation energy plot . Notice that the deviation is removed , but, the data fits with two straight lines. These correspond to the value of $\bar{\phi}_{bo}$ 0.93 and 0.63V and Richardson constants 0.99 x 10^6 and 1.69 x 10^6 $Am^{-2}K^{-2}$. Similarly, the temperature dependence of ideality factor (η_{ap}) can be understood on the basis of equation (3.7). It indicates that $1/\eta_{ap}$ vs 1/T plot should yeild a straight line with slope giving $\sigma_o q\xi/k$ and intercept (1-γ). The increase of η with fall in temperature arises due to the term containing ξ (i.e., the rate of change of σ with bias) . The plot of $1/\eta_{ap}$ vs 1/T also contains two straight lines . Both correspond to negative slopes making ξ essentially negative;the values being -2.38mV and-0.14mV in the temperature range 80-135K and 150-300K, respectively.

It may be mentioned that the studies on many other simultaneously fabricated diodes revealed slight variation in the values of the mean barrier height and standard deviation at zero bias. Such observations are primarily attributed to the local chemistry and conditions of the interface.

3.4 Evidence for a Double Distribution

Figure (3.7) shows yet another lnI vs V characteristics of a Schottky diode fabricated after annealing at 400°C for 1h in vacuum. These clearly depict increasingly linear behaviour over several orders of current and shift towards higher bias side with decrease in temperature . The variation of apparent barrier height and ideality factor with temperature as obtained in this case are given in figures (3.8) and (3.9) respectively. According to equation (3.7) , the plot of ϕ_{ap} should be a straight line with intercept at the ordinate determining the zero bias mean barrier height $\bar{\phi}_{bo}$ and the slope giving the zero bias standard deviation σ_o. However, when the ϕ_{ap} vs 1/T plot is made (figure (3.10)) , data fits nicely , as in the previous case , with two straight lines(transition occurring $\sim$ 135K), implying thereby that $\bar{\phi}_{bo}$ and σ_o assume different values in the temperature range 165-300K and below 165K. The intercepts and slopes of these straight lines yield values of $\bar{\phi}_{bo}$ and σ_o as 0.93V and 0.112V in 165-300K and 0.629V and 0.067V below 165K. ϕ_{ap} can now be estimated from equation (3.7) itself over entire temperature range 80-300K for each set of $\bar{\phi}_{bo}$ and σ_o values. This is presented in figure (3.11) by continuous curves.

Similarly , $1/\eta_{ap}$ vs 1/T plot should also possess different characterstics in the two temperature ranges if contact contains two barrier heights distribution. This is indeed the case as data fits with two straight lines in the temperature ranges 300-165K and below 165K (see ,e.g. , figure (3.12)). Their slopes yield $q\sigma_o\xi/k$ and intercepts at the ordinates give (1-γ) . The value of ξ extracted from the slopes are -2.4mV and -0.14mV whereas the values of γ obtained from the intercepts are -0.75 and 0.187.

Figure (3.13) shows the conventional activation energy $\ln(I_s/T^2)$ vs 1/T plot . The experimental data are seen to fit asymptotically with a straight line at higher temperatures only. The zero bias barrier height obtained from the slope of this straight line comes out to be 0.34V . Likewise the value of Richardson

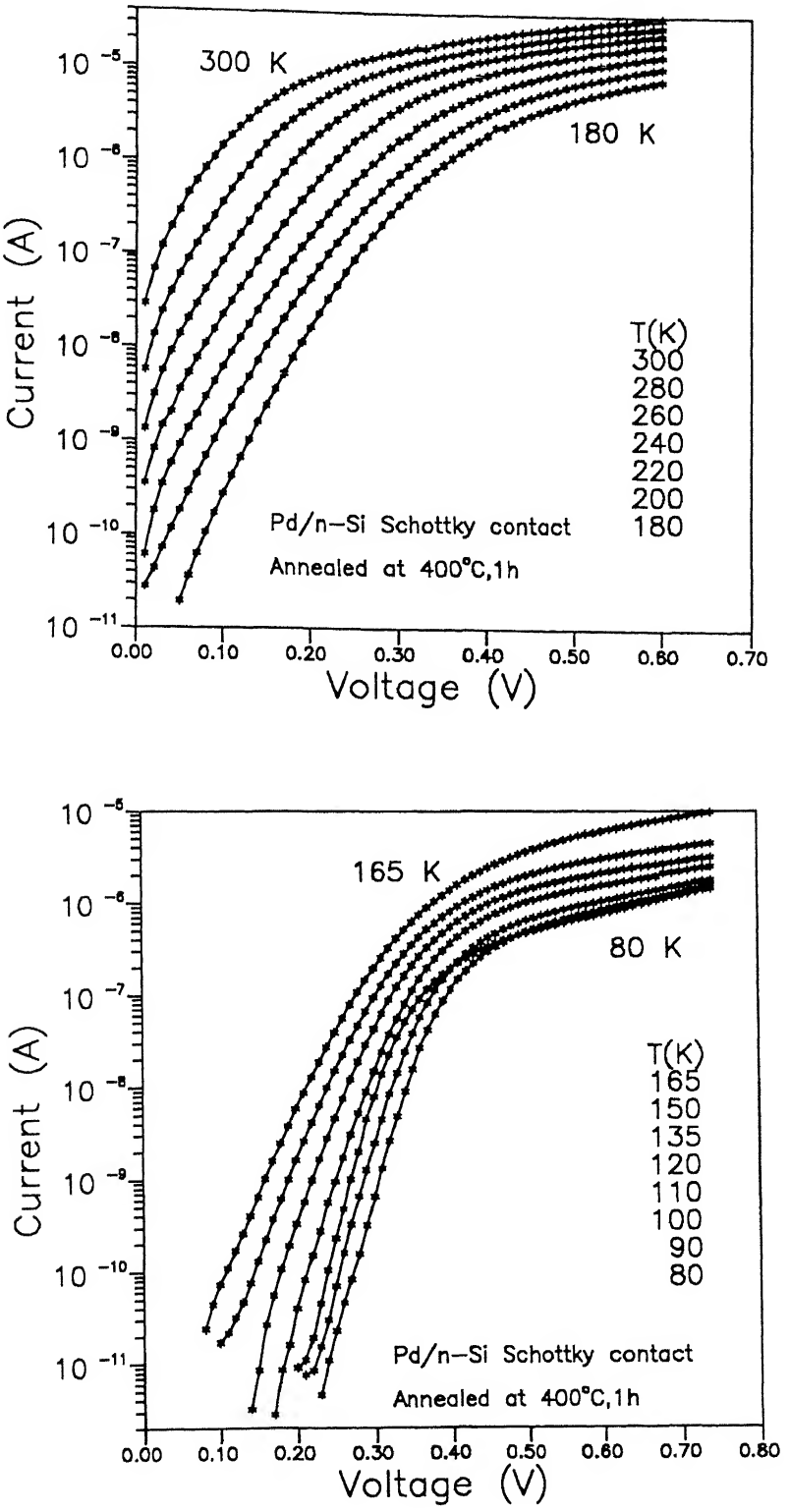

Figure 3.7: Current - voltage characteristics of Pd/n-Si Schottky contacts formed by annealing at 400°C for 1h,in the temperature range (a) 300-180K (b) 165-80K.

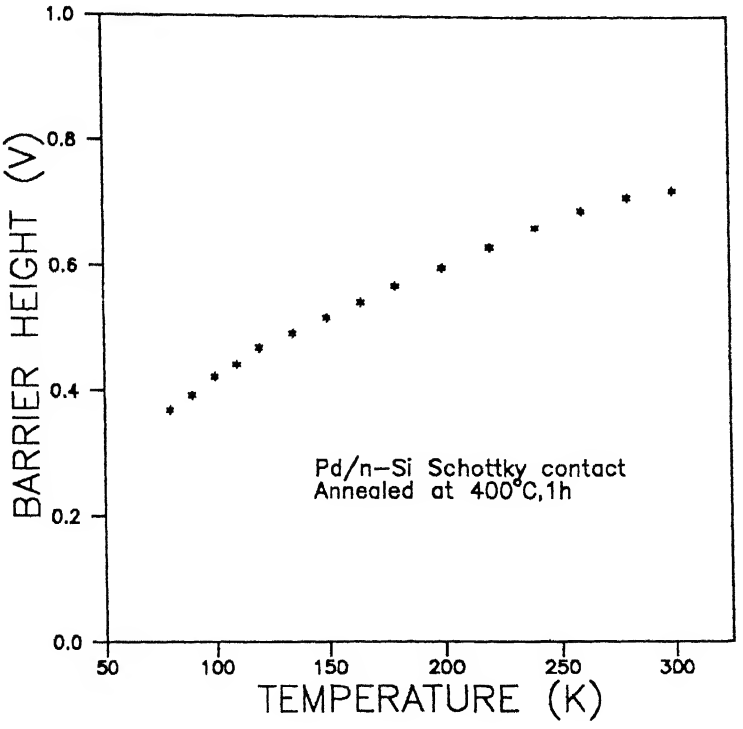

Figure 3.8: Variation of the zero bias barrier height (ϕ_{bo}^{-}) with temperature ,in the range 80-300K.

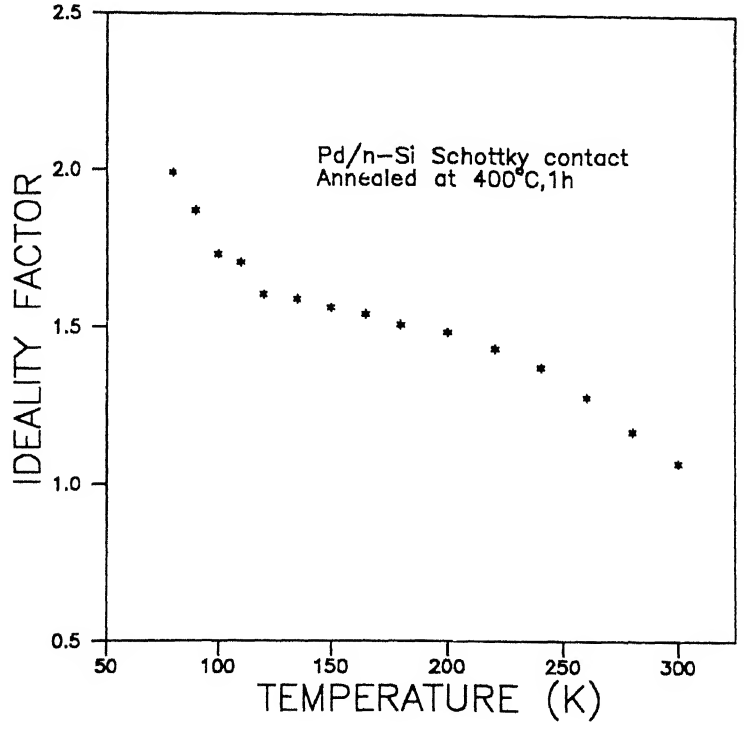

Figure 3.9: Temperature dependence of Ideality factor for Pd/n-Si Schottky contacts ,in the range 80-300K. Notice the sharp increase in η at low temperatures.

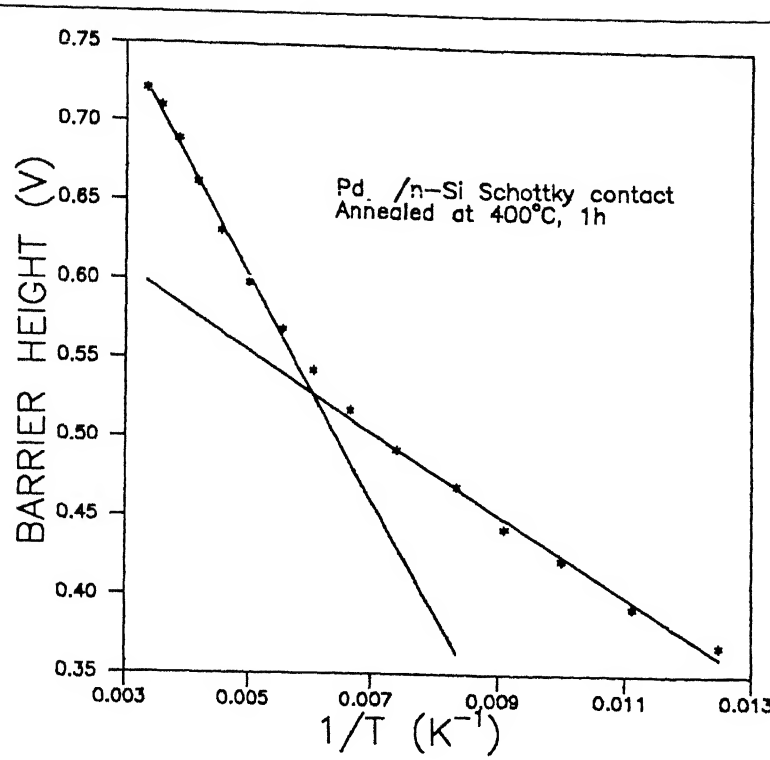

Figure 3.10: The barrier height (ϕ_{bo}) obtained from I-V measurements as a function of inverse temperature.Notice the transition occuring around 150K.

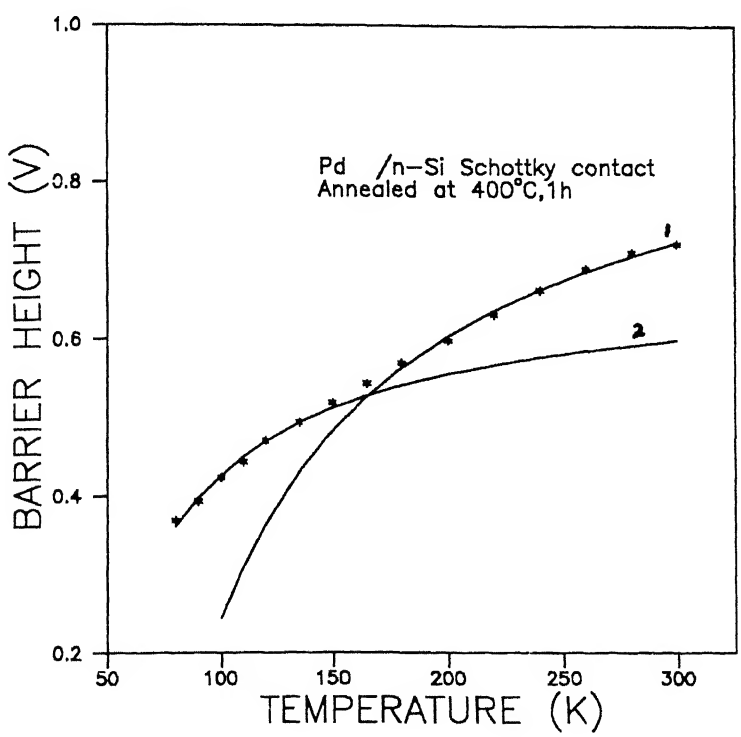

Figure 3.11: The zero-bias barrier height as a function of temperature.Full curves 1 and 2 correspond to ϕ_{ap} calculated using equation (3.8)for two distributions having ϕ_{bo} (0.93V and 0.629V) and σ_o (0.112V and 0.0667V).

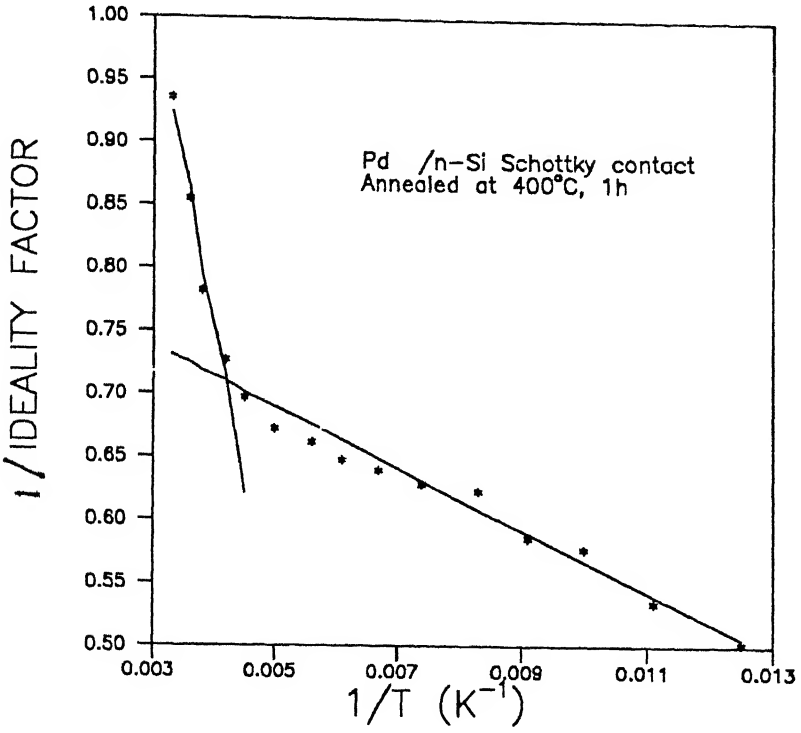

Figure 3.12: The inverse ideality factor($1/\eta_{ap}$) versus inverse temperature (1/T) plot. The data show linear variation in the two temperature ranges with transition around 200K

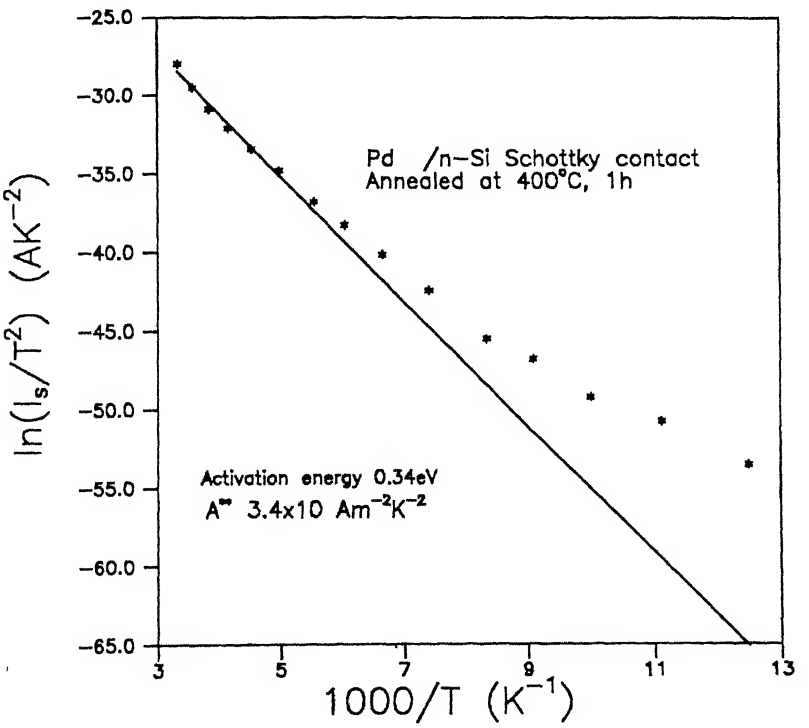

Figure 3.13: Conventional activation energy $\ln(I_s/T^2)$ vs 1000/T plot. Notice the deviation from linearity below 180K.

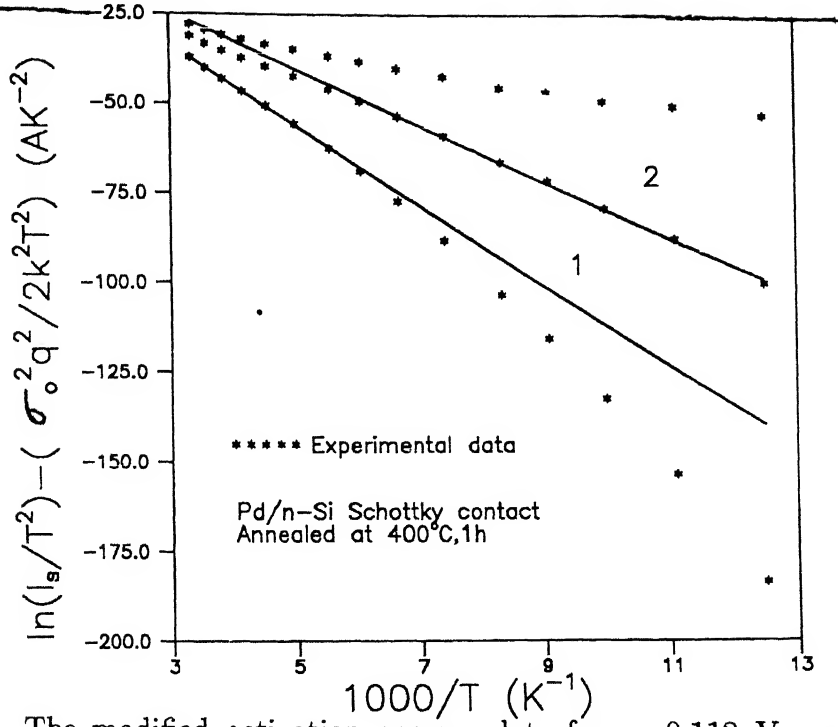

Figure 3.14: The modified activation energy plots for σ_o 0.112 V and 0.067 V , together with the experimental data. The straight lines 1 and 2 indicate best fitting of data in temperature ranges 165-300K and 80-150K , respectively.

constant determined from the intercept at the ordinate is 3.34x10 $Am^{-2}K^{-2}$. Both these parameters are quite unreasonably low as the reported value of the barrier height for Pd_2Si/nSi Schottky diodes is 0.735V [48] and Richardson constant for n-type silicon is 1.12x10^6 $Am^{-2}K^{-2}$ [4] . Moreover, the activation energy plot shows nonlinearity at low temperatures. To explain these discrepancies the I-V data are interpreted in terms of equation (3.10) and a modified activation energy plot (figure (3.14)) is made. For this the term $\ln(\frac{I_s}{T^2}) - \frac{q^2\sigma_o^2}{2k^2T^2}$ is calculated for both the values of σ_o (associated with the Gaussian distributions of barrier heights) found above and then plotted as a function of inverse temperature . The best linear fitting yields zero bias mean barrier heights as 0.969V and 0.680V which match exactly with the mean barrier heights obtained from the ϕ_{ap} vs 1/T plots earlier. The intercept at the ordinate is just ln(A_d A^{**}) and gives Richardson constant A^{**} as 1.22x10^6 $Am^{-2}K^{-2}$ and 1.69x10^6 $Am^{-2}K^{-2}$ for the two straight lines drawn.

All the considerations above suggest that the obsersved experimental data can be satifactorily explained by assuming the existence of two Gaussian distributions

of barrier heights in the present Pd_2Si/nSi Schottky diodes.

3.5 X-ray Diffraction Studies

Fig. (3.15),(3.16),(3.17),(3.18), and (3.19) show X-ray diffractograms of growing silicide at different stages of annealing at 200°C , 400°C ,450°C and 500°C . These are recorded with CuKα radiation(wavelength $\lambda = 1.5418$ $\AA$) at the same sensitivity and time constant. The Bragg angles(2θ) , d-values and relative intensities of various reflections are summarized in Table (3.1) and (3.2) for palladium and palladium silicide , respectively. Palladium film corresponds to f.c.c. phase with a=3.89$\AA$ [41]. The diffraction data suggests that annealing of Pd/n-Si<111> at 400-500°C invariably leads to silicide of composition Pd_2Si having Fe_2P structure with hexagonal unit cell ; the parameters being a=13.055$\AA$, c=27.490$\AA$ [41]. Also ,there is a tendency of preferred orientation , e.g. , at 500°C , Pd_2Si grains assume preferred orientation such that their basal plane lies parallel to (111) of silicon substrate. (Notice appearance of 00.16 reflection and progressive increase in its intensity with annealing) . This means <111> Si is parallel to <00.1> Pd_2Si. This result is consistent with the findings of Buckley and Moss [3]. Further, at 400°C and 450°C , the intensities do not match with the ASTM data [44] of polycrystalline Pd_2Si and therefore indicate the presence of preferred orientation. The diffraction data suggests that (22.8) Pd_2Si lie parallel to (111) Si. With lapse of time , some readjustment occurs and grains assume other orientations as well and move towards true polycrystallinity ,i.e., Pd_2Si exhibits epitaxy in the begining but turns into polycrystalline disposition as it thickens.

Palladium reacts with silicon in accordance with the equation $2Pd + Si \rightarrow Pd_2Si$. Thickness $\tilde{d}$ of Pd_2Si formed can be estimated from

$$\tilde{d}_{Pd_2Si} = \frac{M_{Pd_2Si}\rho_{Pd}}{A_{Pd}N_{Pd}\rho_{Pd_2Si}}\tilde{d}_{Pd}$$

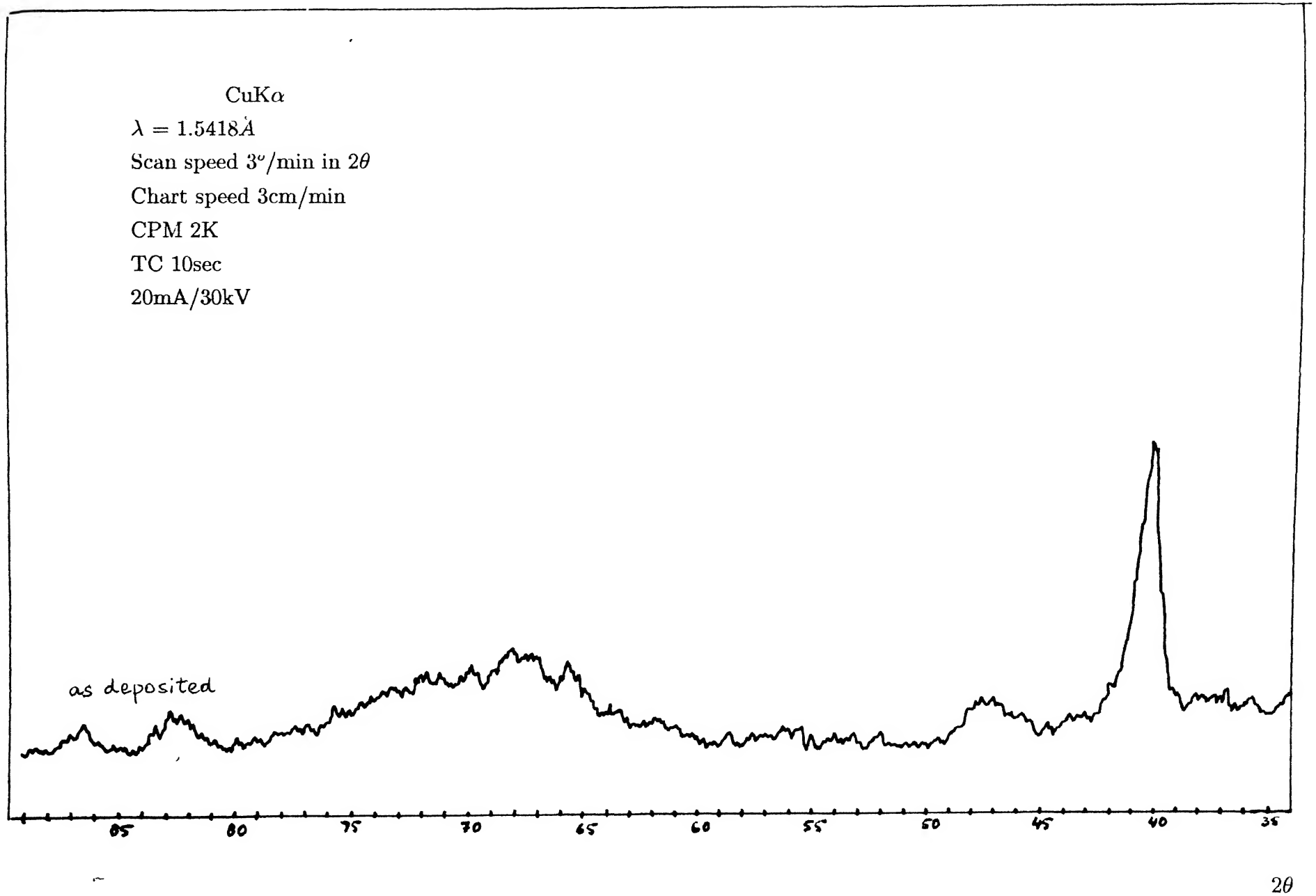

Figure 3.15: Diffractogram for the as deposited sample .

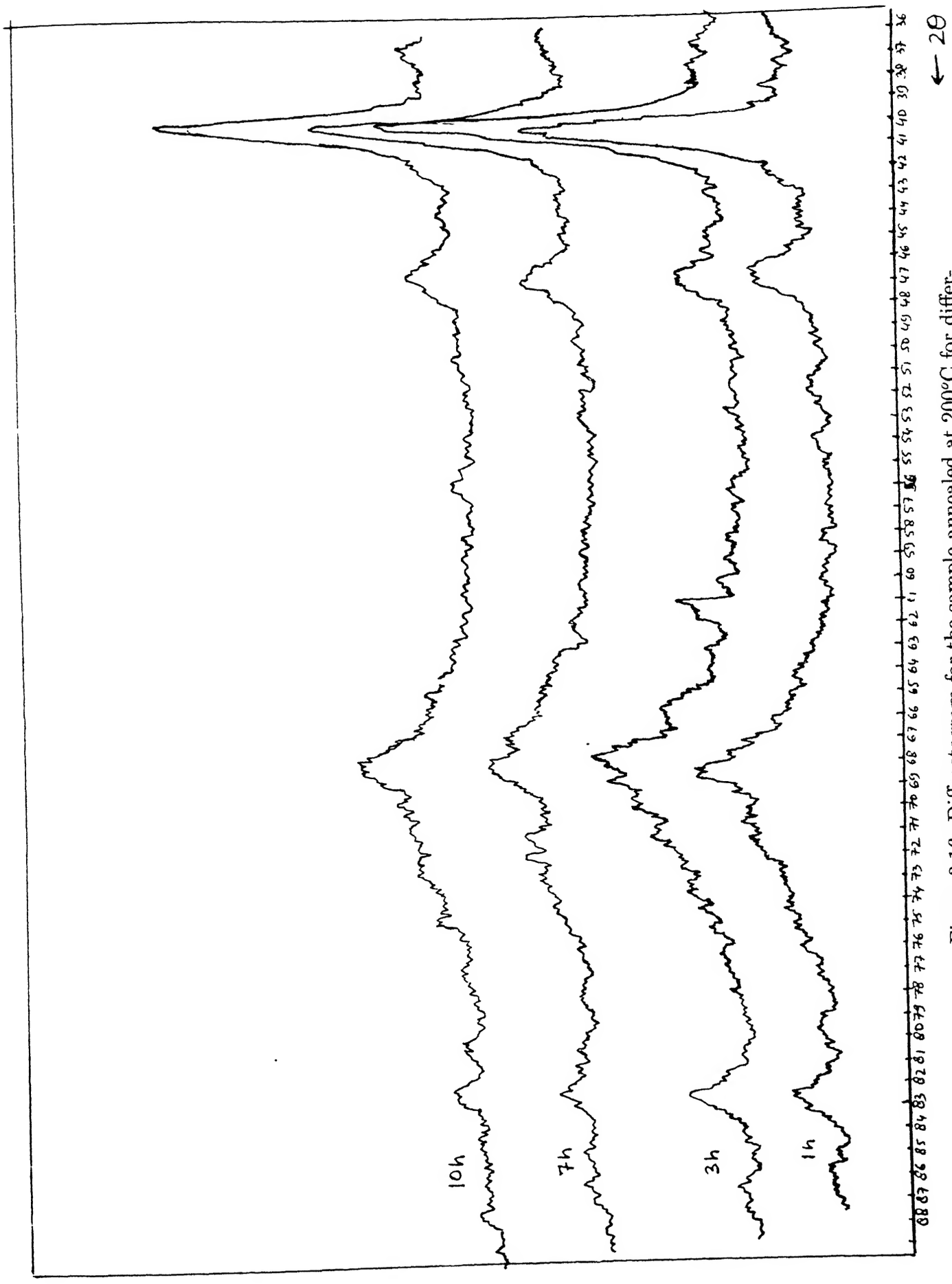

Figure 3.16: Diffractogram for the sample annealed at 200°C for different lengths of time.

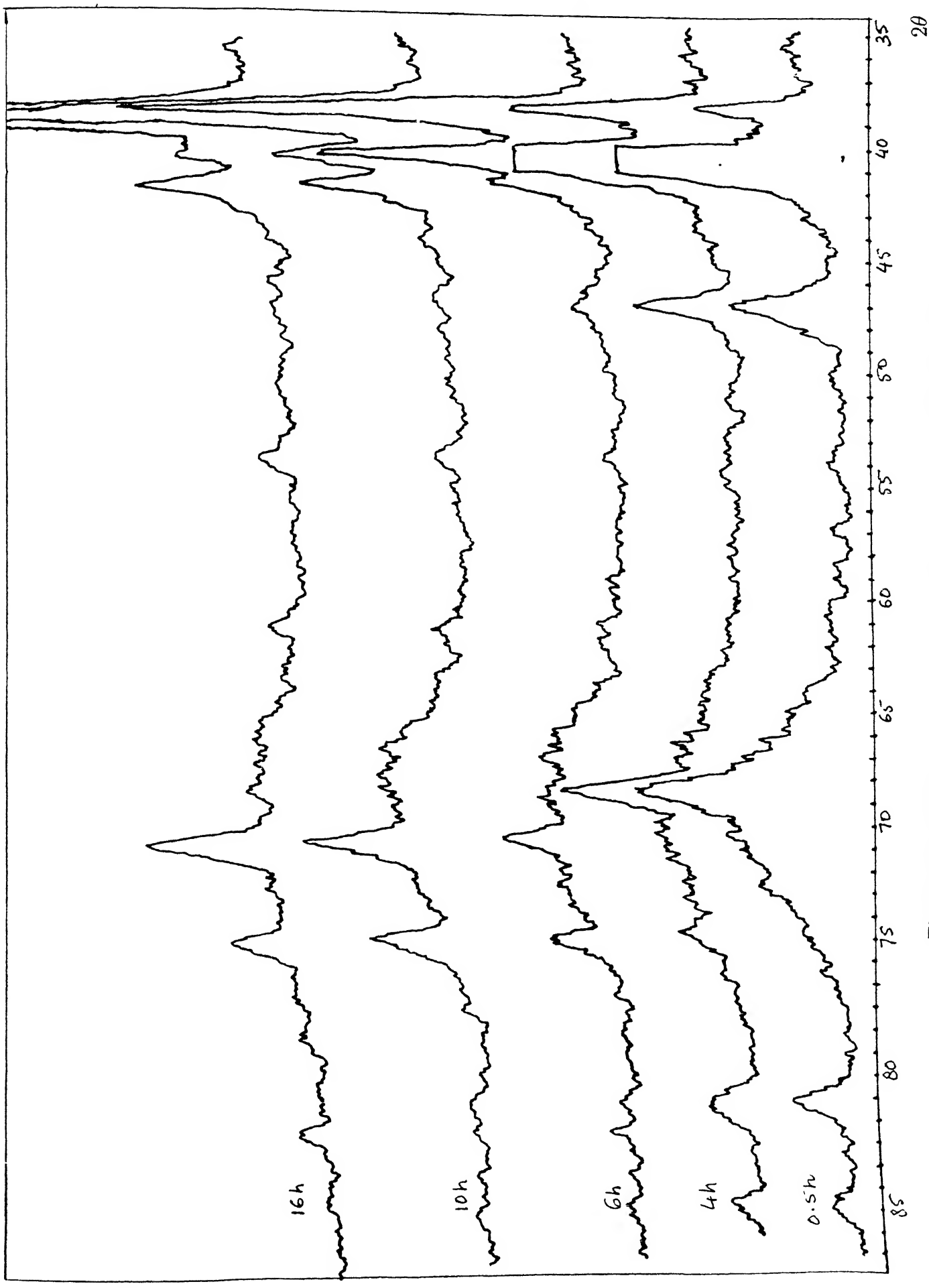

Figure 3.17: Diffractogram for the sample annealed at 400°C for different lengths of time.

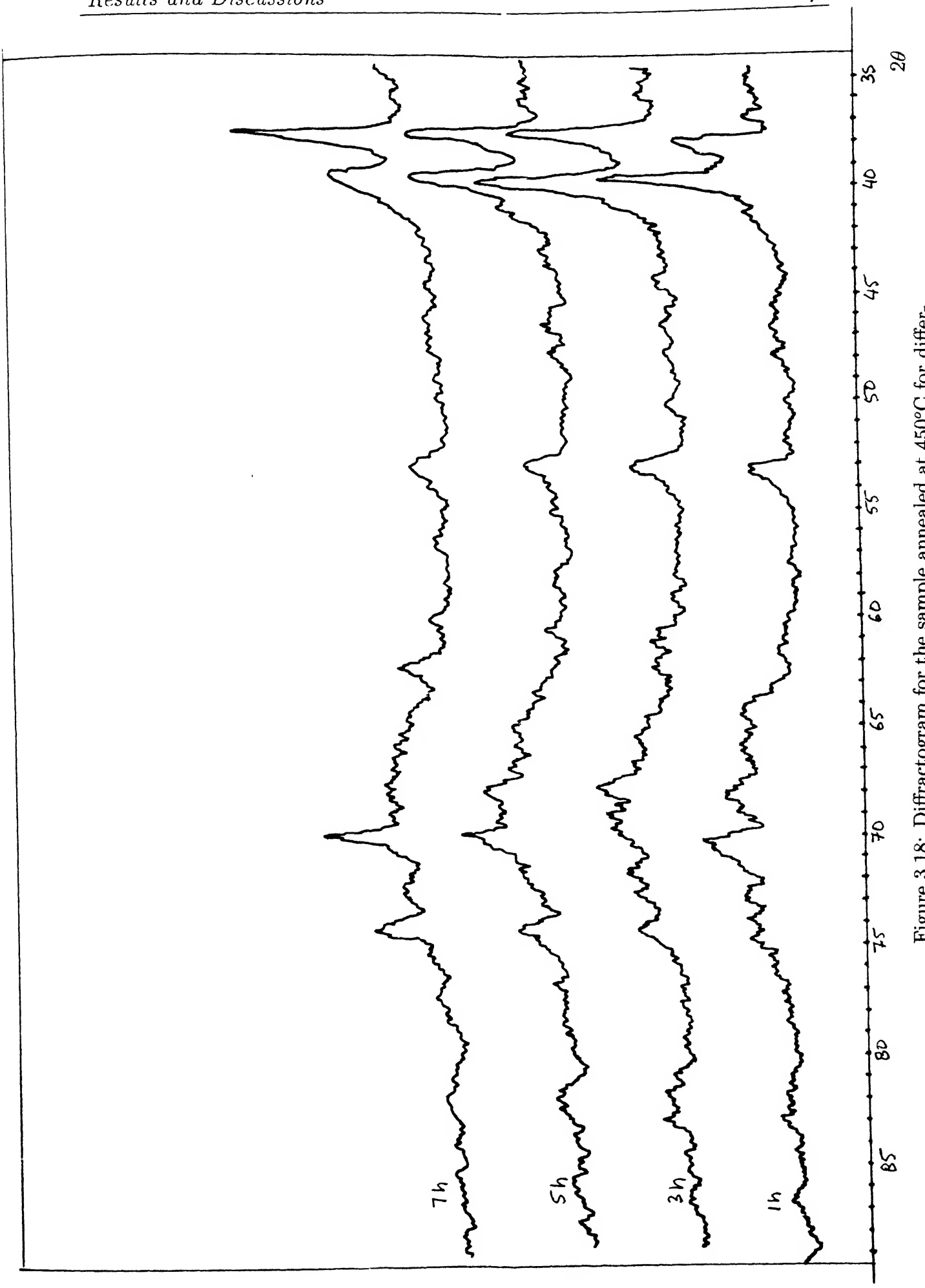

Figure 3.18: Diffractogram for the sample annealed at 450°C for different lengths of time

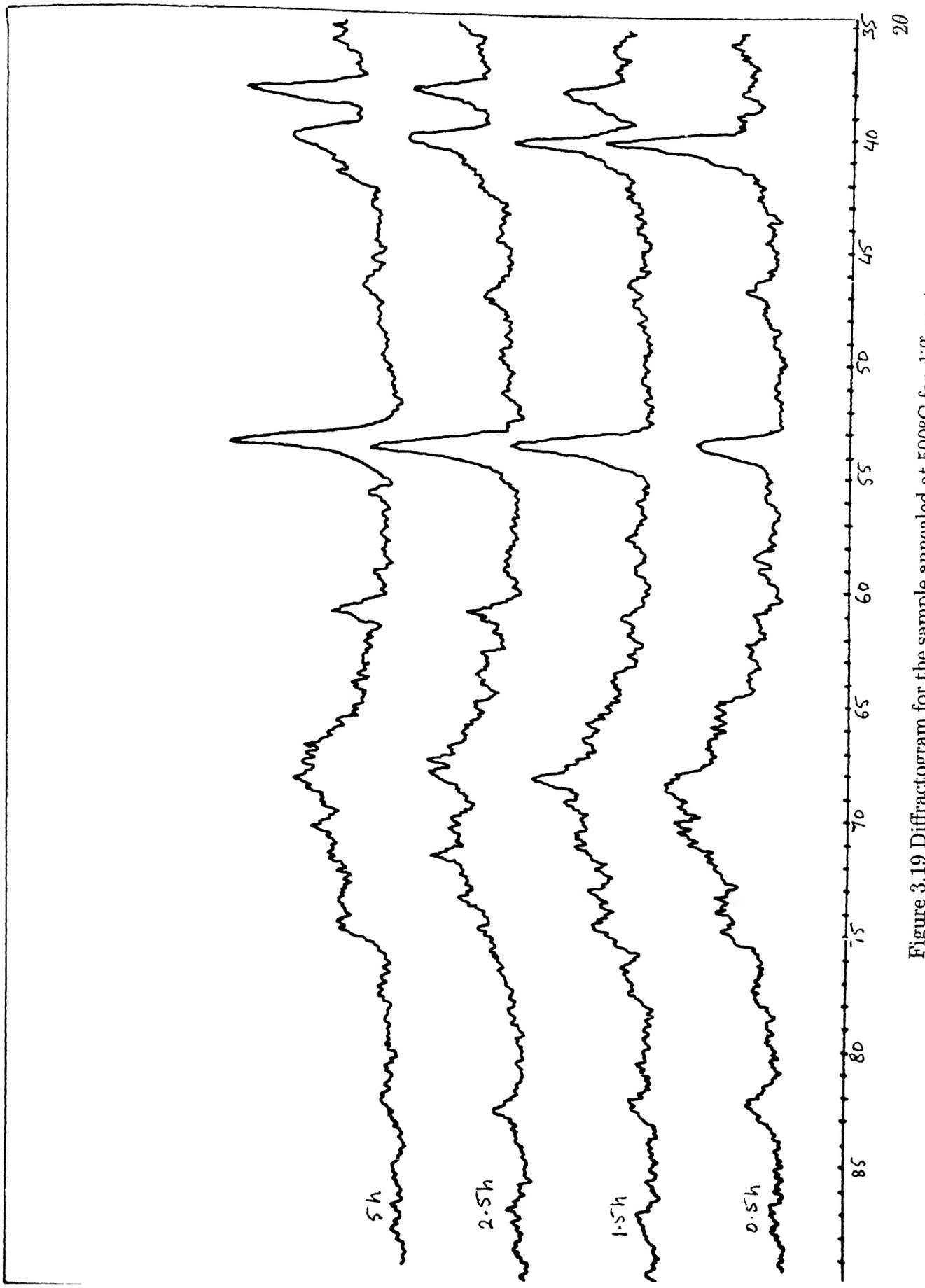

Figure 3.19 Diffractogram for the sample annealed at 500°C for different lengths of time.

Table 3.1: Diffraction peaks for Pd

Pd	Reflections , hkl					
		111	200	220	311	222
as deposited	2θ	40.1	47.1	68.3	82.5	86.6
	d(Å)	2.248	1.930	1.37	1.171	1.122
	R(I)	85	15	30	10	8
annealed	2θ	40.1	47.1	68.3	82.5	86.6
at 200^{O}C	d(Å)	2.248	1.930	1.37	1.171	1.122
1h	R(I)	80	20	40	15	5
	2θ	40.1	47.1	68.3	82.5	86.4
	d(Å)	2.248	1.930	1.37	1.171	1.126
10h	R(I)	80	18	35	10	3
annealed	2θ	40.1	47	68.2	82.4	86.4
at 400^{O}C	d(Å)	2.248	1.933	1.375	1.173	1.126
0.5h	R(I)	180	30	60	20	10
	2θ	40.1	47	-	82.4	-
	d(Å)	2.248	1.933	-	1.173	-
6h	R(I)	80	15	-	10	-
	2θ	40.1	-	-	82.3	-
	d(Å)	2.248	-	-	1.172	-
10h	R(I)	30	-	-	5	-
	2θ	40.1	-	-	-	-
	d(Å)	2.248	-	-	-	-
16h	R(I)	20	-	-	-	-
annealed	2θ	40.1	-	68.2	82.5	-
at 450^{O}C	d(Å)	2.248	-	1.375	1.171	-
1h	R(I)	50	-	28	8	-
	2θ	40.2	-	68.3	82.1	-
	d(Å)	2.246	-	1.373	1.174	-
3h	R(I)	55	-	26	7	-
	2θ	40.1	-	68.1	82.5	-
	d(Å)	2.248	-	1.377	1.171	-
5h	R(I)	40	-	20	5	-
	2θ	40.2	-	-	-	-
	d(Å)	2.246	-	-	-	-
7h	R(I)	20	-	-	-	-
annealed	2θ	40.1	-	68.5	82.3	-
at 500^{O}C	d(Å)	2.248	-	1.369	1.172	-
0.5h	R(I)	50	-	30	10	-
	2θ	40.1	-	68.3	82.5	-
	d(Å)	2.248	-	1.373	1.171	-
1.5h	R(I)	44	-	28	7	-
	2θ	40.2	-	68.8	82.4	-
	d(Å)	2.246	-	1.364	1.1715	-
2.5h	R(I)	39	-	24	5	-
	2θ	40.1	-	68.2	-	-
	d(Å)	2.248	-	1.375	-	-
5h	R(I)	26	-	20	-	-

Table 3.2: Diffraction peaks for Pd_2Si

Pd_2Si	Reflections , hkl						
		228	408	0016	2216	2416	6016
as deposited	2θ	-	-	-	-	-	-
	d(Å)	-	-	-	-	-	-
	R(I)	-	-	-	-	-	-
annealed	2θ	-	-	-	-	-	-
at 200°C	d(Å)	-	-	-	-	-	-
10h	R(I)	-	-	-	-	-	-
annealed	2θ	38.1	-	-	-	-	-
at 400°C	d(Å)	2.362	-	-	-	-	-
0.5h	R(I)	30	-	-	-	-	-
	2θ	38.1	-	53.7	-	-	74.8
	d(Å)	2.362	-	1.709	-	-	1.270
6h	R(I)	140	-	9	-	-	24
	2θ	38	41.5	53.8	-	70.3	74.8
	d(Å)	2.366	2.176	1.703	-	1.339	1.270
10h	R(I)	180	32	10	-	40	26
	2θ	38.1	41.4	53.5	61	70.4	74.9
	d(Å)	2.362	2.181	1.713	1.521	1.337	1.268
16h	R(I)	200	40	12	8	50	30
annealed	2θ	38	-	53.3	-	70.3	-
at 450°C	d(Å)	2.366	-	1.718	-	1.339	-
1h	R(I)	25	-	10	-	24	-
	2θ	38.1	-	53.3	-	70.3	74.9
	d(Å)	2.362	-	1.718	-	1.339	1.268
3h	R(I)	35	-	12	-	23	5
	2θ	38	-	53.4	-	70.4	74.8
	d(Å)	2.366	-	1.715	-	1.337	1.270
5h	R(I)	40	-	11	-	23	10
	2θ	38.1	-	53.3	-	70.3	74.9
	d(Å)	2.362	-	1.718	-	1.339	1.268
7h	R(I)	60	-	12	-	30	16
annealed	2θ	-	-	53.7	-	70.3	-
at 500°C	d(Å)	-	-	1.706	-	1.339	-
0.5h	R(I)	-	-	25	-	18	-
	2θ	38	-	53.4	-	70.4	-
	d(Å)	2.366	-	1.715	-	1.337	-
1.5h	R(I)	20	-	38	-	19	-
	2θ	38.1	-	53.5	60.9	70.4	-
	d(Å)	2.362	-	1.713	1.521	1.337	-
2.5h	R(I)	24	-	42	14	19	-
	2θ	38.1	41.5	53.3	60.9	70.3	74.9
	d(Å)	2.362	2.176	1.718	1.521	1.339	1.268
5h	R(I)	37	5	47	15	18	10

where M_{Pd_2Si} and A_{Pd} are the molecular weight of Pd_2Si and atomic weight of Pd , respectively, ρ_{Pd} and ρ_{Pd_2Si} their densities , $\tilde{d_{Pd}}$ thickness of Pd-film is determined by optical interferometry as $\sim$1050 $\pm$ 50Å. Substituting the values of various paramaters as M_{Pd_2Si}=240.89 , A_{Pd}=106.4 , N_{Pd} = 2 , ρ_{Pd} = 12.02g/cm^3 ρ_{Pd_2Si} = 9.462g/cm^3 , $\tilde{d_{Pd_2Si}}$ is estimated as 1510 $\pm$ 70Å.

Wittmer and Tu [49] have shown that the growth of Pd_2Si on silicon wafer of <100> and <111> orientations is diffusion limited with activation energy (E_a) lying in the range 1.3-1.5 eV. Also, Pd_2Si follows parabolic growth law(i.e., $\tilde{d}$ = $2(Dt)^{1/2}$, where $\tilde{d}$ is the silicide thickness, t is the annealing time and $D(T)=D_o$ exp ($-E_a/kT$) is the chemical interdiffusion constant; the value of D_o is 0.48 or 0.18 cm^2/sec for p-doped Si <100> or <111> orientation) and is independent of the substrate orientation.The rate limiting step is interdiffusion through the silicide layer rather than the interfacial reaction . Further, the dominant diffusing species is palladium in Pd_2Si via vacancies.

These observations are at variance with the earlier reports of Cheung and Nicolet [51] who found diffusion constants to be in the range 10^{-15}- 10^{-13} cm^2/s at 240°C and activation energy of Pd_2Si formation as 0.9$\pm$0.1eV. Our value of interfacial diffusion constant lie in the range 2.2-6.3 x 10^{-15} cm^2/s at 400-500°C and are closer to the later case.

3.6 Reflectance measurements and SEM studies

Fig. (3.20) , (3.21), (3.22) show reflectance(%R) of Pd/n-Si system as such and after annealing for different lengths of time at 400, 450 and 500°C, respectively. Accordingly at 400°C, the reflectance spectra preserve the trend but decreases with time of annealing . On careful examination, it was found that patches of Pd_2Si developed first at a number of places , they enlarged to islands and eventually covered the entire area by coalescence. At 450 °C , the reflectance (%R) decreases

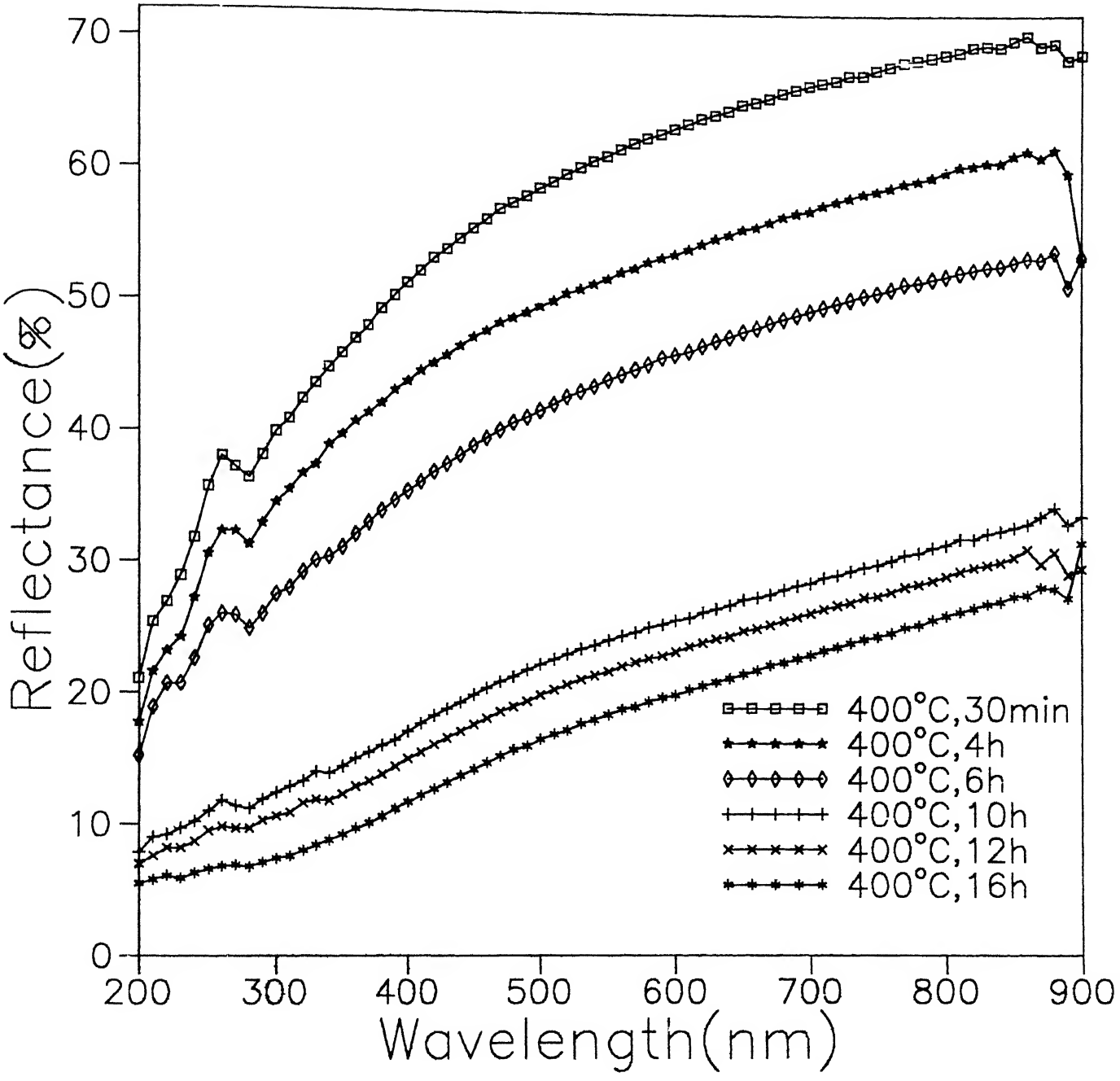

Figure 3.20: Reflectance versus wavelength plots for the sample annealed at 400°C for different lengths of time

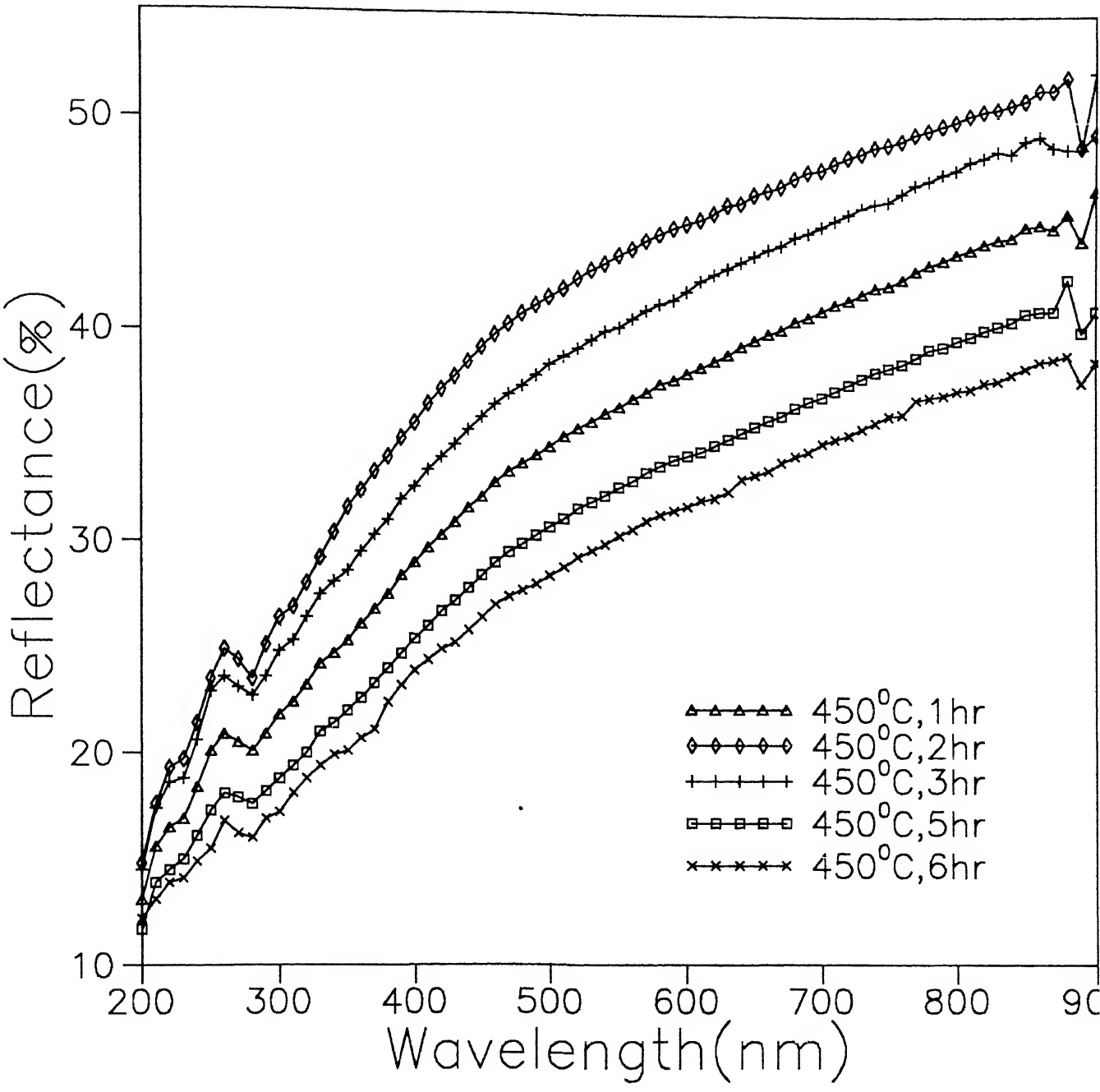

Figure 3.21: Reflectance versus wavelength plots for the sample annealed at 450°C for different lengths of time

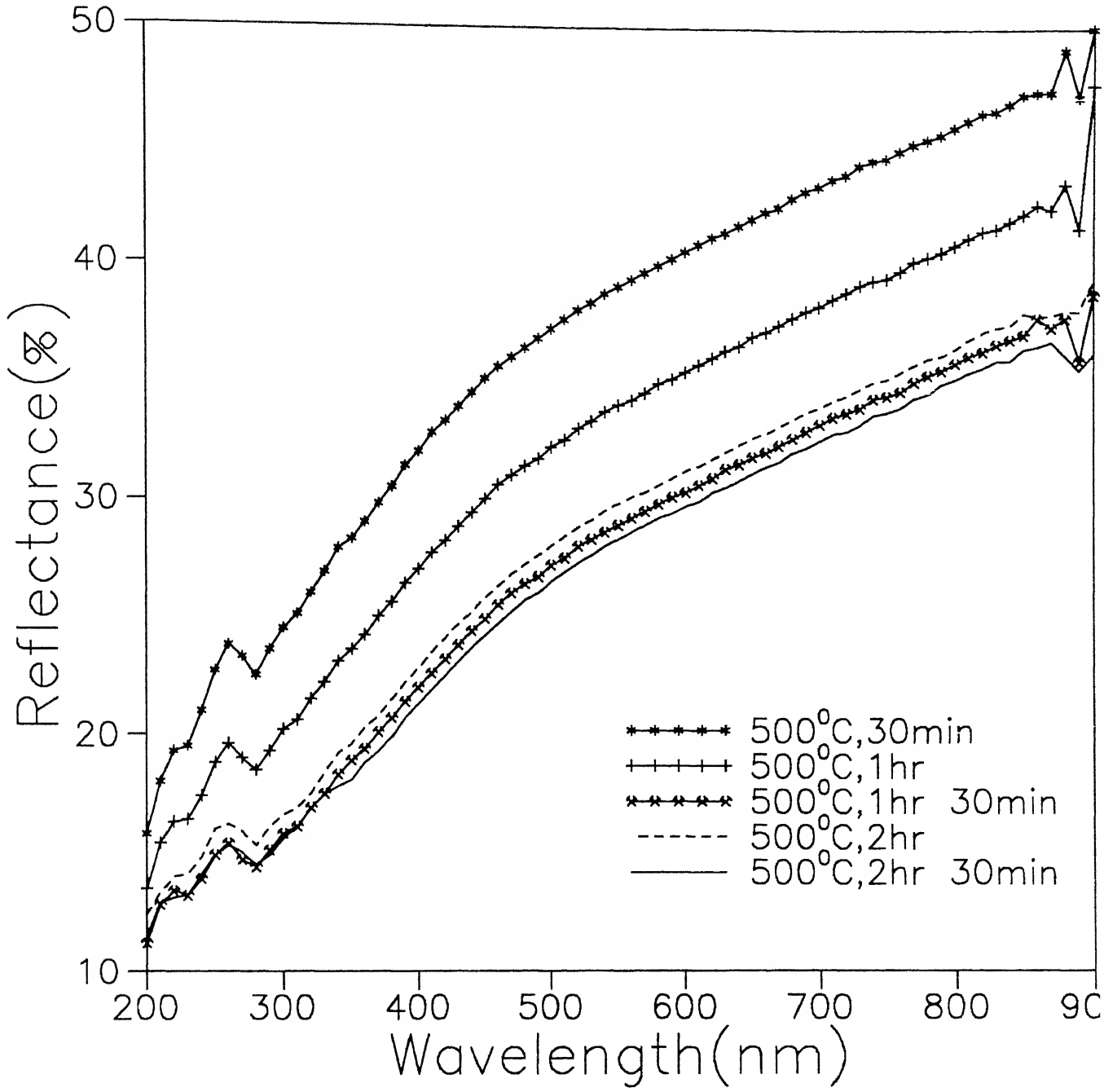

Figure 3.22: Reflectance versus wavelength plots for the sample annealed at 500°C for different lengths of time

initially , then increases upto 2h and eventually decreases at all wavelengths. In this case no patches , as observed at 400 °C , were found . Instead it is believed that lateral growth of Pd_2Si occurs. While the first decrease can be attributed to initial growth of Pd_2Si , the increase in the reflectance may be due to recrystallization and emergence of preferred orientations. As the time lapses , Pd_2Si exhibits increased polycrystallinity (section 3.5) and so reflectance decreases as usual. At 500 °C , reflectance decreases with annealing time as basal plane (00.1) is predominantly lying parallel to the underlying (111) plane of silicon . But , after 1.5h , there is a slight increase in reflectance presumably due to other orientation developing. Eventually randomization occurs and we observe decrease of reflectance after 2.5h.

The scanning electron micrographs are shown in fig(3.23)

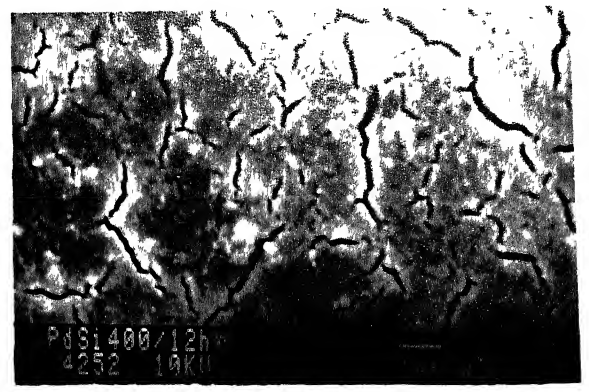

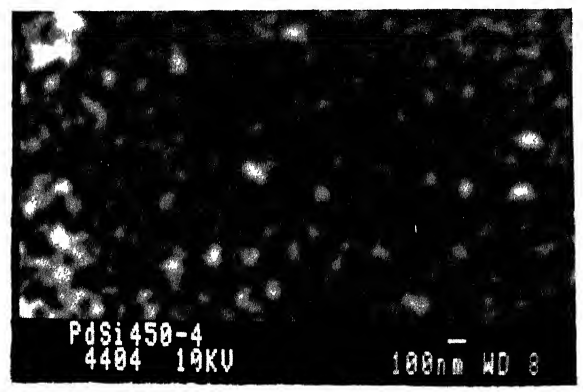

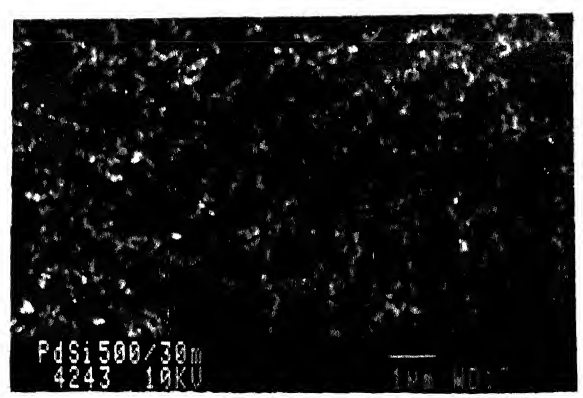

Figure 3.23: Scanning electron micrographs of Pd/n-Si Schottky contacts showing microstructure (a)after annealing at 400°C for 12h (b) after annealing at 450°C for 4h (c) after annealing at 500°C for 30 min.

Chapter 4
Simulation Studies

4.1 I-V characteristics

In order to understand the relative contributions of various current mechanisms, in Schottky diodes, I-V characteristics have been simulated for all of them using known parameters.For this, thermionic emission-diffusion, generation-recombination and tunneling processes are chosen.The thermionic emission-diffusion current through a Schottky diode under a forward bias of V volts is given by [4,7].

$$I_{te} = I_s[exp\,(\frac{qV}{kT}) - 1] \tag{4.1}$$

with saturation current I_s given by

$$I_s = A_d A^{**} T^2 exp(\frac{-q\phi_b}{kT}) \tag{4.2}$$

where A^{**} is the Richardson constant ($1.12 \times 10^6 Am^{-2}K^{-2}$) and ϕ_b is the barrier height (for $Pd_2Si/n-Si$ contact, its value is $\sim$ 0.735eV [11]) . A_d is diode area (for 1mm size dot $A_d = 7.85 \times 10^{-7} m^2$) and k the Boltzmann constant is $1.38 \times 10^{-23} J/K$. With these parameters, I_s has been simulated using eqn(4.2) at various temperatures in the range 50K-300K. For each I_s , in turn , thermionic emission-diffusion current (I_{te}) can be computed from eqn(1.10) at various forward bias levels at the corresponding temperature. Figure 4.1 shows the results ln(I) vs (V) plots at various temperatures. Notice that saturation current I_s lies in the region $\sim 10^{-36}A - 10^{-9}A$ at temperatures 100K - 300K.

The generation-recombination current through a Schottky diode under forward bias of V volt is given by [4].

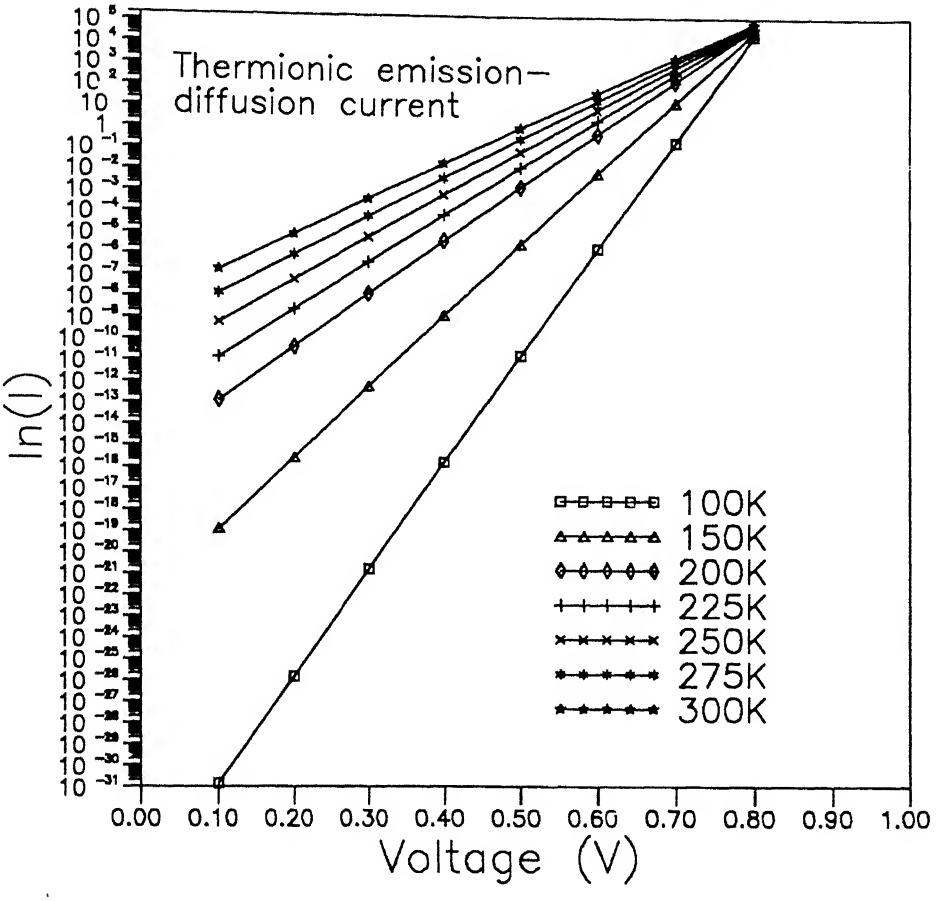

Figure 4.1: Simulated ln(I) vs V plots for the current due to thermionic emission-diffusion process at different temperatures

$$I_r = I_{ro}[exp\{\frac{qv}{2kT}\} - 1] \tag{4.3}$$

with saturation current current

$$I_{ro} = qn_i wA_d/2\tau \tag{4.4}$$

where, n_i is the intrinsic carrier concentration, w is the width of the depletion region, A_d is the area of the junction(interface) andτ is the carrier life time. n_i is given by [7]

$$n_i = 2[\frac{2\pi k}{h^2}]^{3/2}[m_e^* m_h^*]^{3/4}T^{3/2}exp[\frac{-E_g}{2kT}] \tag{4.5}$$

where m_e^* and m_h^* are the effective mass of the electron and hole respectively that have value 1.18m and 0.81m ; m being the mass of electron , E_g is the band gap of silicon,k the Boltzmann constant and h is the Plank's constant . The value of n_i is determined at different temperatures with $E_g = 1.12$eV , w = $0.3\mu m$, $A_d = 7.85\times10^{-7}m^2$ and $\tau = 10^{-6}$s [7].Generation recombination current can be obtained from eqn(4.3) and eqn(4.4) at different temperatures (Fig.4.2). Notice that the saturation current is always 2-5 orders of magnitude less than the corresponding values obtained for the TED process (Fig.4.1).

The tunneling current through the barrier under a forward bias of V volt is given by [4,12,13]

$$I_t = I_{to}exp(V/E') \tag{4.6}$$

with the saturation current I_{to}

$$I_{to} = \frac{A^*T(\pi qE_{oo})^{1/2}}{k}\left\{\left(qV + \frac{q\phi_b}{cosh^2\frac{qE_{oo}}{kT}}\right)^{1/2} exp(\frac{-\phi_b}{E_o})\right\} \tag{4.7}$$

and every parameter

$$E' = E_{oo}\{(\frac{qE_{oo}}{kT}) - tanh(\frac{qE_{oo}}{kT})\}^{-1} \tag{4.8}$$

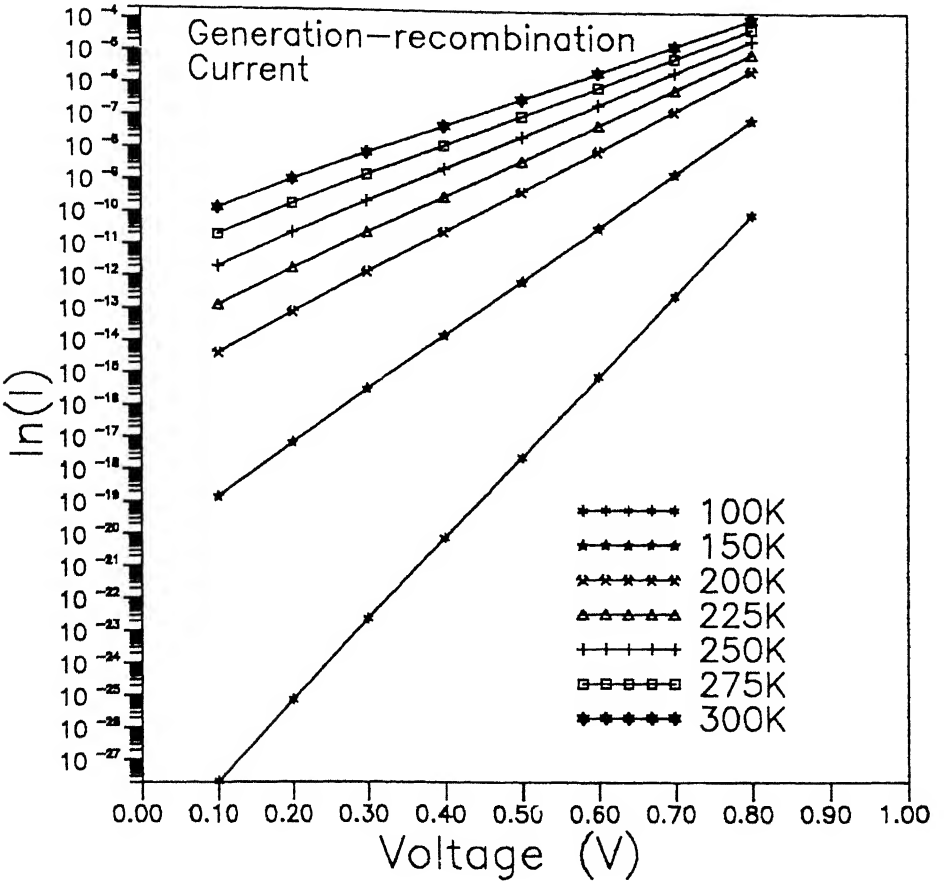

Figure 4.2: Simulated ln(I) vs V plots for current due to generation recombination process at different temperatures

E_o and E_{oo} are related such that

$$E_o = E_{oo} coth \frac{qE_{oo}}{kT} \tag{4.9}$$

withE_{oo} given by

$$E_{oo} = \frac{h}{4\pi}(\frac{N_d}{m_e^* \epsilon_s})^{1/2} \tag{4.10}$$

where N_d is the donar density and ϵ_s is permittivity of silicon. At donar concentration $N_d \sim 1.35 \times 10^{21}, m_e^* = 1.18m$ and $\epsilon_s = 11.9$, E_{oo} comes out to be 1.88×10^{-4} eV. Using this value of E_{oo}, E' can be calculated at different temperatures and in turn,I_{to} with $A^* = 1.12 \times 10^6 AK^{-2}\bar{m}^2, \phi_b = 0.763eV$.Thus,tunneling current is obtained at different bias from eqn(4.6) for temperature range 50K-300K . Fig(4.3) shows variation of tunneling current with bias at various temperatures.The plots reveal very little variation of current with bias. Also,the current level drops down significantly with decrease in temperature. Fig (4.4) shows bias dependance of current more clearly at 300K. Obviously, tunneling current is always very low in comparison to current resulting due to TED and generation recombination processes.(See eg., Fig (4.5)).

The ln(I)-V plots should be linear for all the three currents as per the governing equations (4.1),(4.3),(4.6).It has however been observed that the experimental ln(I)-V plots are linear over several orders of current,higher biases.Such an effect is actually caused by the series resistance (R_s) present.In this situation , bias applied to the diode gets modified to (V-IR_s)in equations(4.1)(4.3)(4.6) Saturation effects appear and the current can be estimated by iteration only as described in chapter 3.Also,fitting of I-V data in TED current equation gives barrier height ϕ_{ap} and η.It is usually found that ϕ_{ao} decreases and η increases with decrease in temperature and activation energy plot deviates from linearity at low temperatures.It amounts to saying that the actual current is more than the contribution made by TED process itself. These anomolies are at first sight indicate a deviation from the thermionic

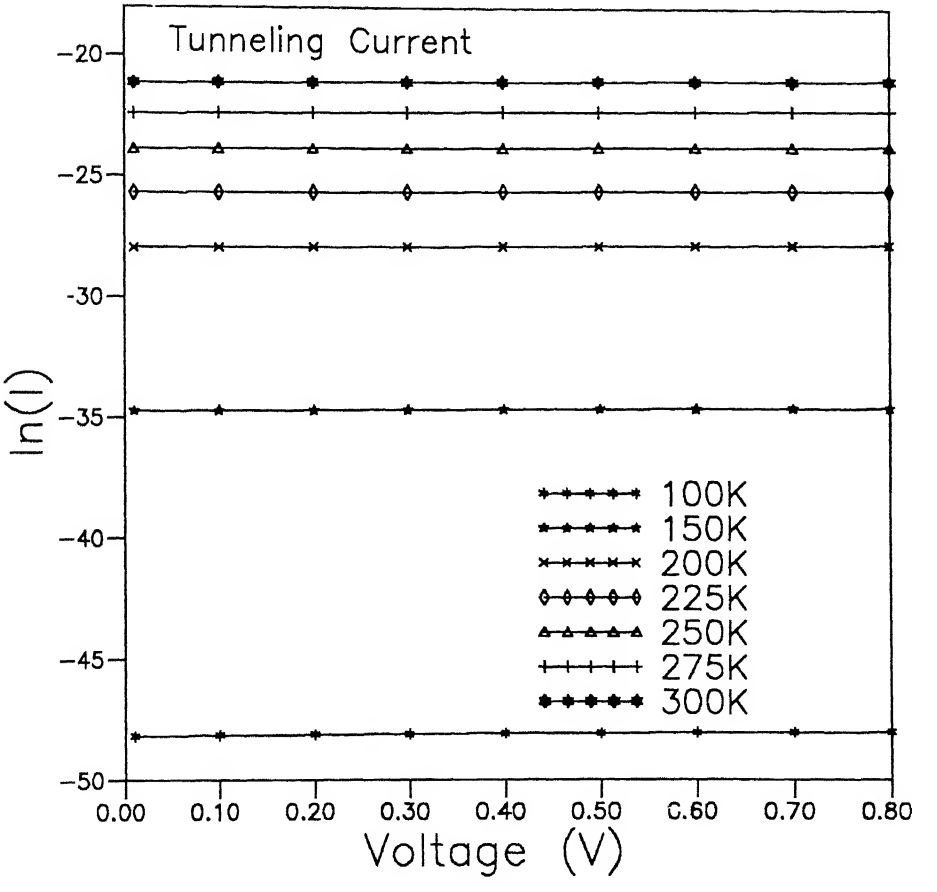

Figure 4.3: Simulated ln(I) vs V plots for the current due to tunneling process at different temperatures

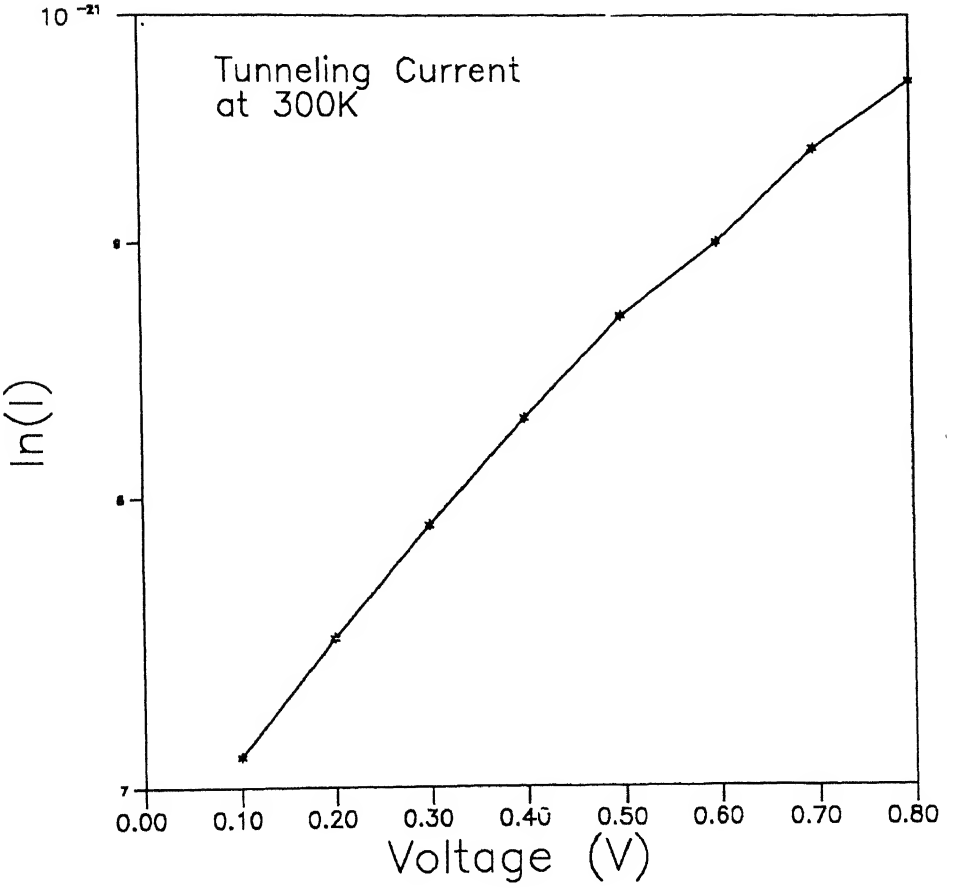

Figure 4.4: Simulated ln(I) vs V plots for the Tunneling process at 300K

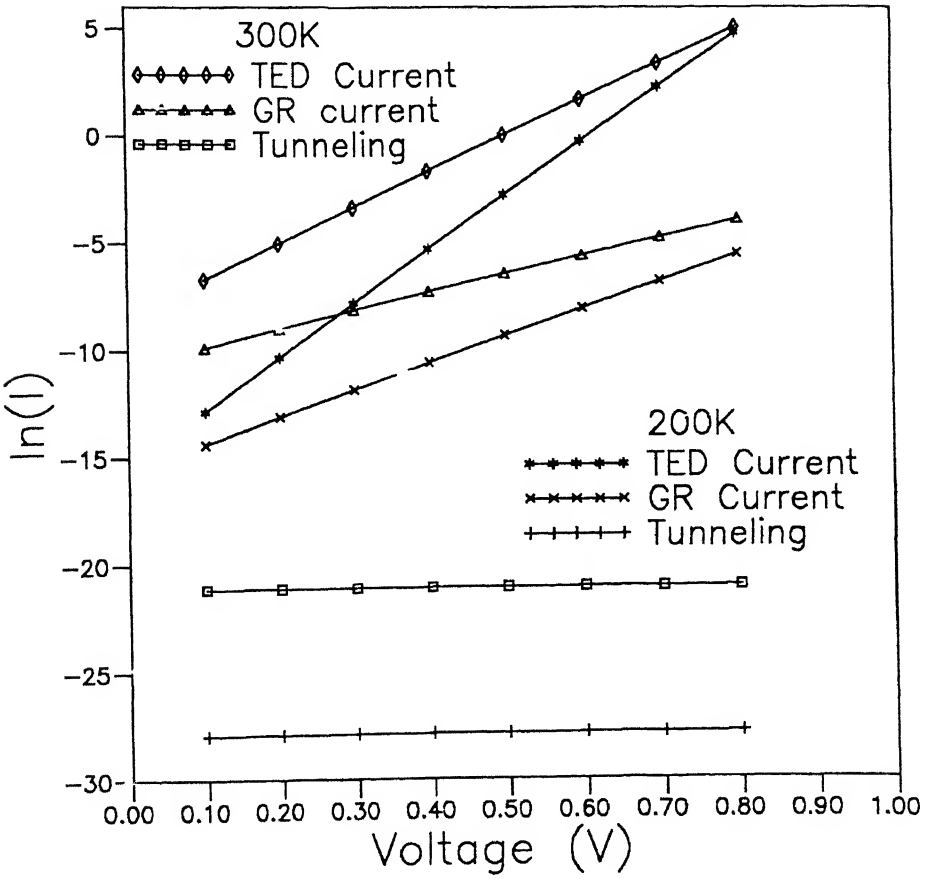

Figure 4.5: Simulated ln(I) vs V plots showing the current due to the three mechanisms simultaneously at 300K and 200K

emission-diffusion mechanism.The possible reason could be the simultaneous operation of other processes viz.,tunneling through the barrier or recombination in the depletion region.

The tunneling involves field emission and thermionic field emission through the barrier.The process applicable,however, depends upon the parameter

$$E_{oo} = \frac{h}{4\pi}(\frac{N_d}{m_e^*})^{1/2} = 18.5 \times 10^{15}(\frac{N_d}{m_e \epsilon_r})^{1/2} eV \qquad (4.11)$$

The field emission becomes important when $E_{oo} \gg kT/q$,whereas thermionic field emission (TFE)dominates when $E_{oo} \sim kT/q$ and thermionic emission-diffusion if $E_{oo} \ll kT/q$ [4]. In the present case $E_{oo} = 0.188$mV with $N_D = 1.35 \times 10^{21} m^{-3}$, $m_s = 1.1$ and $\epsilon_s = 11.9$.This leads to qE_{oo}/kT equal to 0.0071 at 300K and 0.027 at 80K . Obviously , the condition prevailing in both the situations is $E_{oo} \gg kT/q (\sim 0.259mV$ and $\sim 0.7mV$ at 300K and 80K, respectively) and hence the possibility of FE and TFE can be easily ruled out.The tunneling current as estimated from eqn. comes out to be very low $\sim 10^{-21}$A at 300K and $\sim 10^{-47}$A at 100K, whereas, the experimentally obtained values just at forward bias of 0.1V are 10^{-6}A and 10^{-11}A at 300K and 100K respectively.

The second mechanism , i.e. , the generation and recombination requires (see ,e.g., eq(4.3)) the ideality factor to be close to 2.But this value of η is found at 80K. Below 80K,the η remains much smaller than 2.The saturation current calculated using eqn(4.4),comes out to be $\sim 10^{-12}$ Amp at 300K and 10^{-30} A at 100K.Obviously the estimated current values for recombination process are excessively low compared to those actually observed in experiments.Chen et al [52] have pointed out that if recombination current exists,the barrier height evaluation on the basis of TED theory yields progressively lower values with decrease in temperature;for example,if I_r constitute 91% of the total current at (say) 100K,barrier decrease expected is

$$\bar{\phi_{ap}} = \bar{\phi_{bo}}(0) - \frac{q\alpha_2}{2k} + \alpha_1 T - \frac{q\sigma_o^2(0)}{2k} \cdot \frac{1}{T} \tag{4.15}$$

Thus, $\bar{\phi_{ap}}$ contain terms amounting to direct and inverse temperature dependence. The above equation is used to determine $\bar{\phi_{ap}}$ in the temperature range 50K-350K for different values of α_1 and α_2. For this data taken are $\bar{\phi_{bo}}(0K) = 0.8$V and $\sigma_o(0) = 0.06$V. The value of α_1 is varied from -0.3mV/K to +0.3mV/K and that of α_2 from -3$(mV)^2$/K to +3$(mV)^2$/K.

Notice the coefficient α_2 is for variance σ_o^2. The corresponding values of temperature coefficient of standard deviation lie in the range -0.025mV/K to +0.25mV/K . Fig.(4.5) shows the variation of apparent barrier height as a function of temperature at various values α_1 when α_2 is equal to zero. The situation with $\alpha_1 = 0$ corresponds to equation(4.12) itself. It depicts decrease of barrier height with decrease in temperature due to the presence of Gaussian distribution of barrier heights with mean($\bar{\phi_{bo}}$) and variance (σ_o^2) . When $\bar{\phi_{bo}}$ itself varies with temperature (i.e., α_1= -3 to 3 mV/K and α_2= 0) the extent of decrease is reduced or enhanced depending upon the sign of temperature coefficient(i.e., positive or negative). The difference is , however, more prominent at higher temperatures ,i.e., above 150K.

The effect of α_2 on the barrier height is just opposite and shown in Figs.(4.6) and (4.7) for α_1= -3mV/K and 3mV/K, respectively. Here , the extent of decrease is less or more if sign of α_2 is negative or positive. Physically, it means that when α_2 is negative (equivalent to narrowing of the distribution function, i.e., moving towards homogenization of barrier heights) , the decrease of barrier height will be less than predicted by equation(4.12). On the other hand , when α_2 is positive , distribution function widens and amounts to increase in the value of σ_o with rise in temperature . Consequently, there is effectively more reduction in $\bar{\phi_{bo}}$ then determined by equation(4.12).

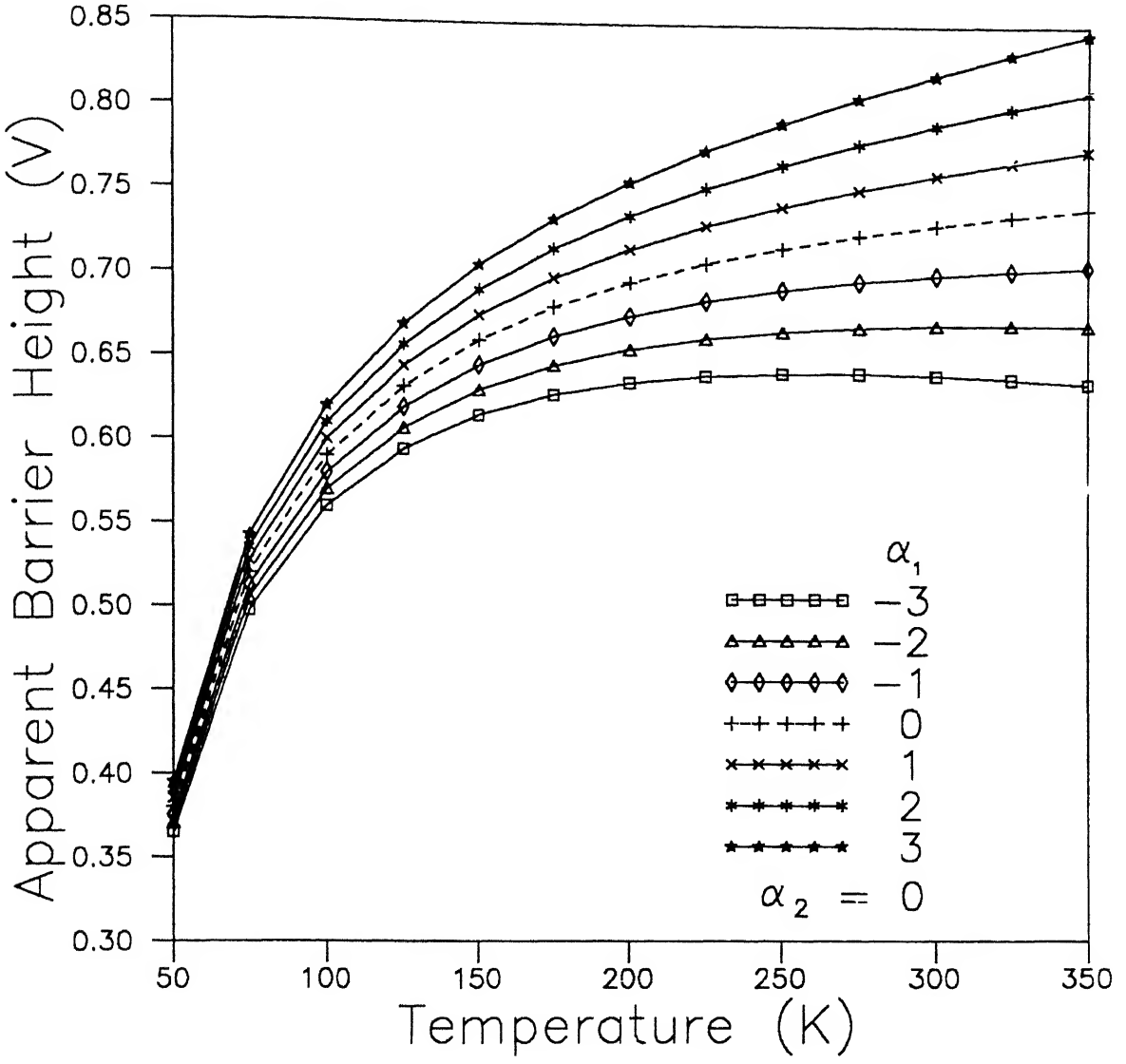

Figure 4.6: Apparent barrier height versus temperature plot with α_1 varying from -3 to 3 mV/K and α_2 zero

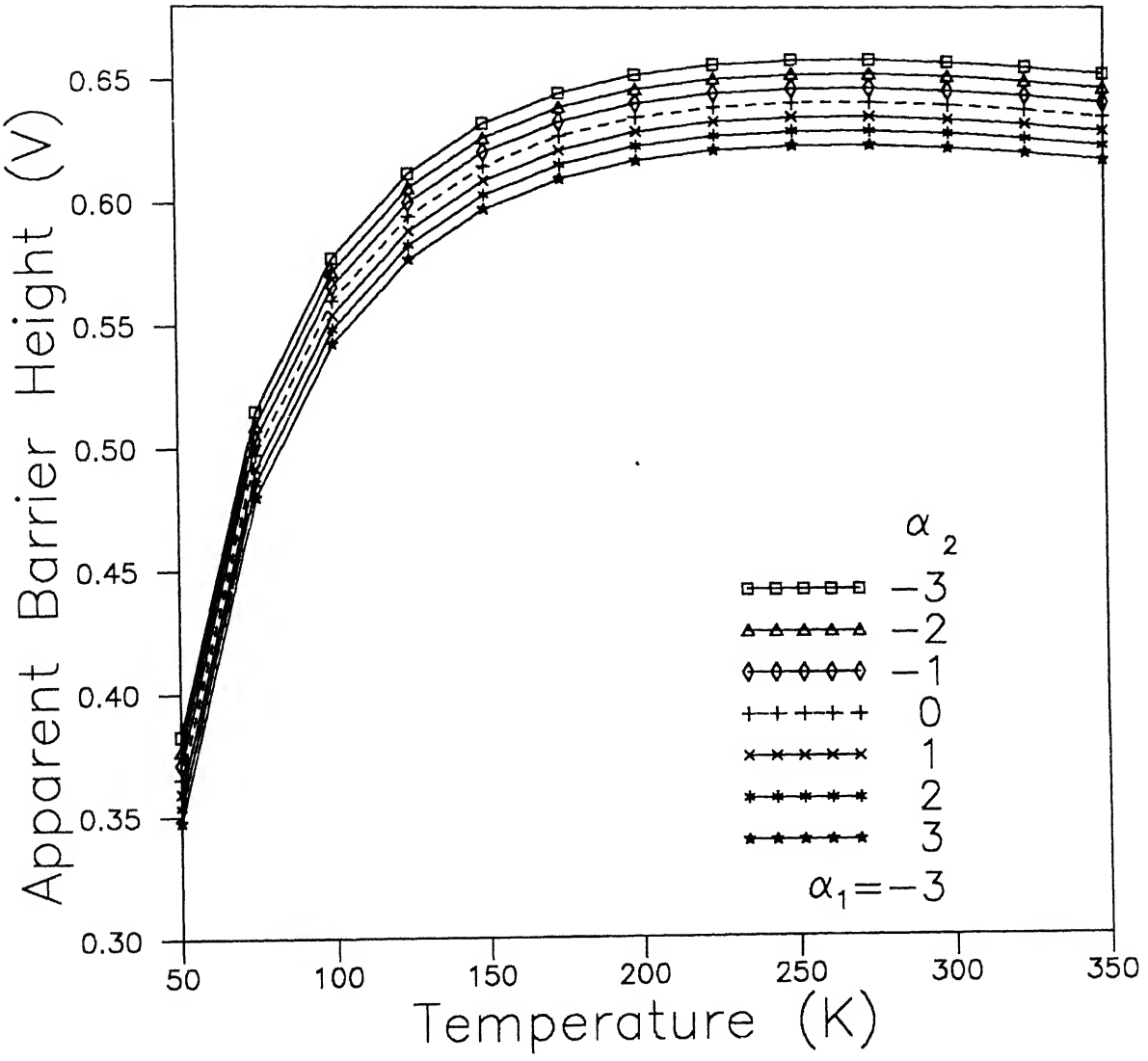

Figure 4.7: Apparent barrier height versus temperature plot with α_1=-3 mV/K and α_2 varying from -3 to 3 mV^2/K

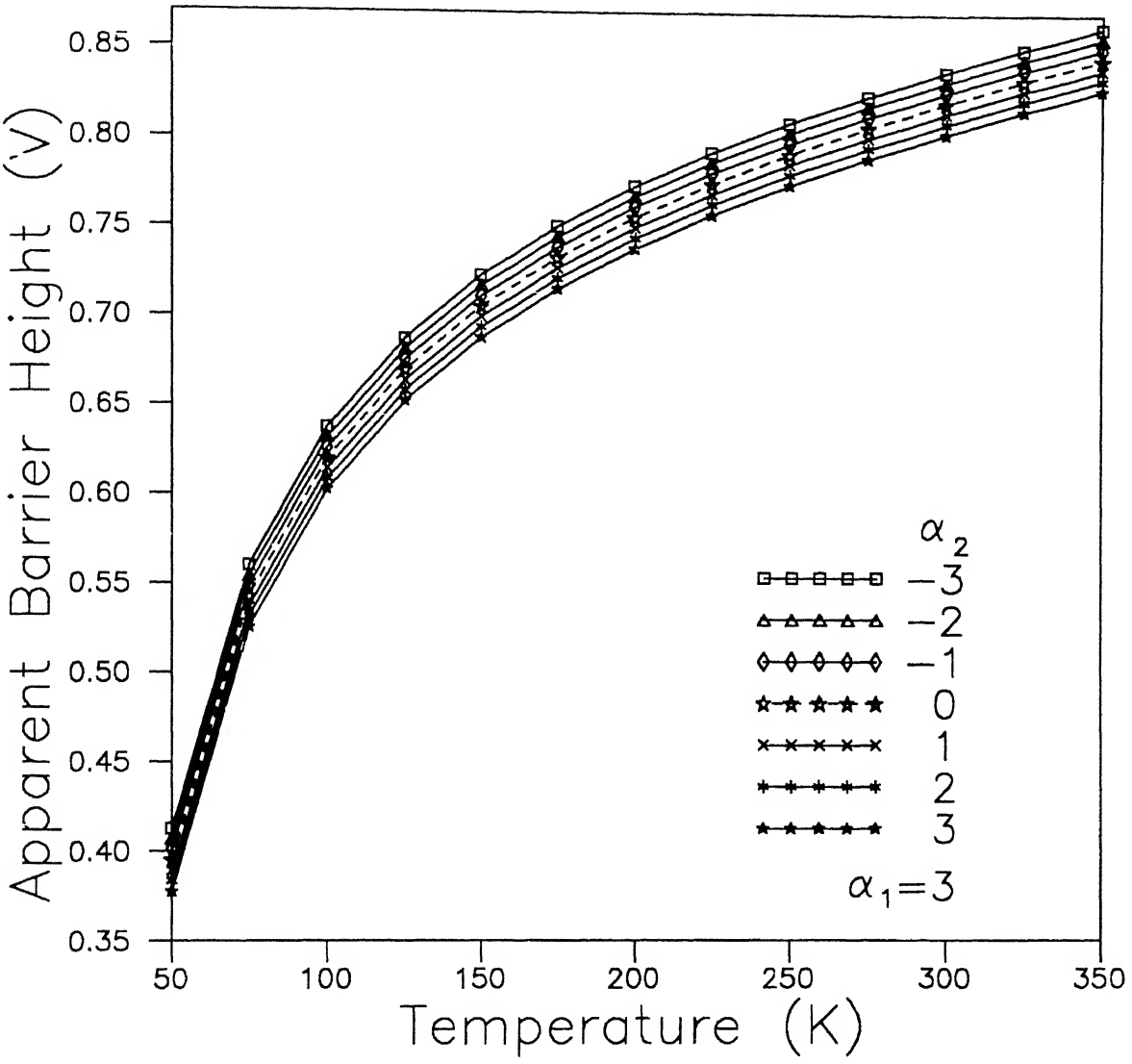

Figure 4.8: Apparent barrier height versus temperature plot with α_1=3 mV/K and α_2 varying from -3 to 3 mV^2/K

Chapter 5
Conclusions

• Pd/n-Si(111) Schottky barrier diodes can be prepared successfully by depositing a palladium layer of $\sim$ 800$\AA$ thickness using an electron beam evaporation source in vacuum $\sim 10^{-6}$ mbar onto a thorougly cleaned silicon substrate.

• I-V characteristics of Pd/n-Si(111) Schottky contacts can be explained on the basis of thermionic emission-diffusion (TED) mechanism . The ln(I) vs V plots over the temperature range (80K-300K) exhibit linearity over several orders of current and saturates due to effectiveness of voltage drop occuring across the series resistance (R_s) of the diode.

• Several diode parameters , viz, barrier height , ideality factor , series resistance and saturation current can be determined by the fitting of the I-V data in the TED current equation using a computer program. While the zero bias barrier height ϕ_{bo} decreases , ideality factor η and series resistance R_s increase with the decrease in temperature. Moreover , the changes in ϕ_{bo}, η , and R_s become quite significant at low temperatures.

• The abnormal behaviour of Pd/n-Si Schottky diodes i.e. , decrease of zero bias barrier height and increase of ideality factor with decrease in temperature can be successfully explained on the basis of TED mechanism by incorporating the concept of barrier inhomogenities and describing them by a Gaussian distribution of barrier heights. The values of parameters obtained are : zero bias mean barrier height (ϕ_{bo}) 0.93V and 0.63V , standard deviation (σ_o) 0.112 and 0.067V in the temperature range (165K-300K) and (80K-165K), respectively.

• The ϕ_{bo} vs 1/T plot yields straight line(s) to demonstrate the number of barrier distribution(s) , viz, single, double or multiple existing at the Schottky

contact giving values of both ϕ_{bo} and σ_o . Similarly, inverse ideality factor $(1/\eta)$ vs inverse temperature (1/T) plot displays linearity and it's intercept at the ordinate and slope determine the bias coefficients (γ and ξ) of the mean barrier height and the standard deviation , respectively.

- The annealing of Pd/n-Si <111> at 400-500°C invariably leads to silicide formation of the composition Pd_2Si having a hexagonal structure (Fe_2P type) with parameters a = 13.055Å , c= 27.490Å. Also, there is a tendency of preferred orientation in the begining but with lapse of time , some readjustment occurs and grains assume other orientations as well to exhibit true polycrystallinity.

- Simulation studies suggest dominance of TED mechanism in the Pd/n-Si Schottky contacts.Also, negative temperature coefficients of mean barrier height $(\bar{\phi_{bo}})$ and variance (σ_o^2) of the Gaussian distribution function (representing the barrier inhomogeneties at the Schottky contact) are found to have opposite effects on the temperature dependence of apparent barrier height. While the former causes decrease in barrier height the later compensates the change by a fixed amount. The overall effect is that Gaussian distribution function shifts towards lower barrier height and at the same time becomes narrower with rise in temperature , i.e., effective reduction in barrier height occurs.

Bibliography

[1] M.S. Tyagi,in Metal-Semiconductor Schottky Barrier Junctions and their Applications, ed. by B.L. Sharma(Plenum,New York 1985)p.1.

[2] F. Braun, Uberdie Stromeleitung durch Schwefelmwtalle,Ann.Phys.Chem. 153,556(1874)

[3] V.L.Rideout, "A review of the theory, technology and applications of metal-semiconductor rectifiers", *Thin Solid Films* **48**, 261-291 (1978).

[4] E.H. Rhoderick, *Metal-Semiconductor contacts*, Clarendon Press, Oxford (1978).

[5] M.A. Nicolet and S.S. Lau, "Formation and characterization of transition-metal silicides" in, *VLSI Electronics Microstructure Science, Vol. 6: Materials and Process Characterization*, N.G. Einspruch and G. Gildenblat (editors), Academic Press, New York, (1983), p 329.

[6] H. Luth, *Surfaces and Interfaces of Solid Materials*, Springer, (1995).

[7] S. M. Sze, *Physics of Semiconductor Devices*, John Wiley and Sons, New York (1981).

[8] H.A.Watson,in H.A.Watson(ed.),*Microwaves semiconductor devices and their circuit applications* McGrawHill,NY(1969) chapters 10-12.

[9] J.C.Irwin and N.C.Vanderwal, in H.A.Watson(ed.) , Microwave semiconductor devices and their circuit applications , Mc Graw Hill , NY(1969) p.349.

[10] V.Heine*Phys.Rev.A***138**,1689 (1965).

[11] C.R. Crowell and S.M. Sze, "Current transport in metal-semiconductor barriers", *Solid-State Electron.* **9**, 1035 (1966).

[12] F.A. Padovan and R. Sttraton, "Field and thermionic-field emission in Schottky barriers", *Solid-State Electron.* **9**, 695 (1966).

[13] C.R. Crowell and V.L. Rideout, "Normalized thermionic-field emission in metal-semiconductor barriers", *Solid-State Electron.* **12**, 89 (1969).

[14] A.Y.C. Yu and E.H. Snow, "Surface effects on metal-silicon contacts", *J. Appl. Phys.* **39**, 3008 (1968).

[15] K.Tada and J.L.R. Laraya, Proc. IEEE, **55** , 2064 (1967).

[16] F.W. Hewlett,*Solid-state circuits*,**10**,343 (1975).

[17] H.H. Berger and S.K.Wiedmann,*IEEE International Solid State Circuits Conf. Tech. digest*,**172**(1975)

[18] H.K. Henisch, *Semiconductors Contacts*, p123. Oxford University Press, London (1984).

[19] A.G.Milnes and D.L.Fencht, *Heterojunctions and Metal-Semiconductor junctions*,Academic Press, New York (1972).

[20] E.H.Rhoderick,*Metal-Semiconductor contacts*,IEEE Proc.,**129** ,1 (1982).

[21] B.L.Sharma and S.C.Gupta *Solid State Technol.***23**,90-97 (1980).

[22] D. Donoval, M. Barus and M. Zdimal, "Analysis of I-V measurements on PtSi-Si Schottky structures in a wide temperature range", *Solid-State Electron.* **34**, 1365 (1991).

[23] V.W.L.Chin, M.A.Green and ›rey, "Evidence for multiple barrier heights in p-type PtSi Schootky-bar‹ ‹iodes from I-V-T and photoresponse measurements", *Solid-State Electron.* **33**, 299 (1990).

[24] M. Wittmer, "Current transport in high-barrier IrSi/Si Schottky diodes", *Phys. Rev. B* **42**, 5249 (1990).

[25] M. Wittmer, "Conduction me‹‹‹‹ism in PtSi/Si Schottky diodes", *Phys. Rev. B* **43**, 4385 (1991).

[26] J.P. Sullivan, R.T. Tung, M.R. Pinto and W.R. ‹ ‹hm, "Electron transport of inhomogeneous Schottky barriers: A numerical study", *J. Appl. Phys.* **70**, 7403 (1991).

[27] M.A.Taubenblatt,D.Thompson and C.R.Helms,*Appl. Phys. Lett.* 44,815 (1992)

[28] M. Barus and D. Donoval, "Analysis of I-V measurements on $CrSi_2$-Si Schottky structures in a wide temperature range", *Solid-State Electron.* **36**, 969 (1993).

[29] M.O. Aboelfotoh, "Temperature dependence of the Schottky-barrier height of tungsten on n-type and p-type silicon", *Solid-State Electron.* **34**, 51 (1991).

[30] M.O. Aboelfotoh, A.Cros B.G.Svensson and K.N.Tu, "Schottky-barrier behavior of copper and copper silicide on n-type and p-type silicon", *Phys. Rev. B* **41**, 9819 (1990).

[31] M.O. Aboelfotoh, "Electrical characteristics of Ti/Si(100) interfaces", *J. Appl. Phys.* **64**, 4046 (1988).

[32] B.Larsson and O.Engstrom,*Semiconductor Sci. and Technol.*, **3**, 572-576 (1988).

[33] V.W.L. Chin, J.W.V. Storey and M.A. Green, "A note on current-voltage measurements of n-type and p-type Pd_2Si Scottky diodes, *Solid-State Electron.* **34**, 215 (1991).

[34] J.H. Werner and H.H. Guttler, "Temperature dependence of Schottky barrier heights on silicon", *J. Appl. Phys.* **73**, 1315 (1993).

[35] S.Chand and J.Kumar,*Semiconductor Sci. and Technol.***10** ,1680 (1995).

[36] S.Chand and J.Kumar,*J Appl.Phys.***80** ,288 (1996).

[37] S.Chand and J.Kumar,*Appl.Phys.A***63**, 171-178 (1996).

[38] S.Chand and J.Kumar,*Semiconductor Sci. and Technol.***11** ,1203-1208 (1996).

[39] S.Chand and J.Kumar,*Semiconductor Sci. and Technol.***12** ,899-906 (1997).

[40] B.D. Cullity, "Elements of X-Ray Diffraction" Addison-Wesley, London (1978).

[41] *Powder Diffraction File Nos.* **5**-681 ; **19**- 893.

[42] T.H.Di Stefano, *Appl. Phys. Lett.* **19**, 280 (1971).

[43] L.J. Brillson, *Surf. Sci. Rep.* **2**, 2 (1982).

[44] E.H. Nicollian and J.R. Brews, *MOS Physics and Technology*, Wiley-Interscience, New York (1982) Chap.6 p 235.

[45] J.H.Werner and H.H.Guttler, Barrier inhomogeneities at Schottky contacts, *J. Appl. Phys.* **69**, 1522 (1990).

[46] Y.P. Song, R.L.V. Meirhaegle, W.H. Laflere and F. Cardon, "On the difference in apparent barrier height as obtained from capacitance-voltage and current-voltage-temperature measurements on Al/p-InP Schottky barriers", *Solid-State Electron.* **29**, 633 (1986).

[47] Subhash Chand,"Experimental and simulation studies of barrier inhomo genities in $Pd_2Si/n-Si$ Schottky diodes"(Ph.D thesis).

[48] M. Wittmer, W. Luthy, B. Studer and Melchion, *Solid-State Electron.* **24**, 141 (1981).

[49] M.Wittmer and K.N.Tu,*Physical Review B***27** , 1173-1179 (1983).

[50] N.D.Buckley and S.C.Moss,*Solid State Electron.***15**,1331 -1337 (1972).

[51] N.W.Cheung , M.A.Nicolet, M.Wittmer, C.A.Evans,Jr., I.I.Sheng *Thin Solid Films***79**, 51-60 (1981).

[52] T.P.Chen ,T.C.Lee,C.C.Ling, C.D. Beling, S. Fung,*Solid State Electron.***36**,949 (1993).